Insight into the critical evaluation indicators for fatigue performance recovery of rejuvenated bitumen under different rejuvenation conditions

Ren, Shisong; Liu, Xueyan; Erkens, Sandra

DOI
10.1016/j.ijfatigue.2023.107753

Publication date
2023

Document Version
Final published version

Published in
International Journal of Fatigue

International Journal of Fatigue 175 (2023) 107753

Contents lists available at ScienceDirect

International Journal of Fatigue

journal homepage: www.elsevier.com/locate/ijfatigue

Insight into the critical evaluation indicators for fatigue performance recovery of rejuvenated bitumen under different rejuvenation conditions

Shisong Ren *, Xueyan Liu, Sandra Erkens

Section of Pavement Engineering, Faculty of Civil Engineering and Geosciences, Delft University of Technology, The Netherlands

ARTICLE INFO

Keywords:
Rejuvenated bitumen
Fatigue life recovery
Rejuvenator type/dosage
Critical evaluation indicators
Potential correlations

ABSTRACT

This study aims to propose critical fatigue indicators for evaluating the restoration effectiveness of various rejuvenators on the fatigue performance of aged bitumen. The influence factors of rejuvenator type/dosage and aging degree of bitumen are involved, and different fatigue parameters from linear viscoelastic (LVE), linear amplitude sweep (LAS), and time sweep (TS) tests are analysed. The results reveal that bio-oil exhibits the greatest rejuvenation efficiency in improving fatigue life of aged bitumen, followed by engine-oil and naphthenic-oil rejuvenators, while aromatic-oil shows the lowest effect. Moreover, the rejuvenation percentages on fatigue parameters of rejuvenated bitumen enhance significantly with increased rejuvenator dosage but weaken as the aging level deepens. The fatigue failure temperature (FFT) from the LVE test, fatigue life (N_{fS}), peak strain (ε_{sr}), elastic modulus (E) from the LAS test, and crack width (C_{500}) from the TS test are recommended as critical indicators for fatigue performance evaluation of rejuvenated binders. Further, the crack width greatly correlates with other essential indicators and can be predicted using correlation equations without conducting the time-consuming time sweep test. The difference in these critical fatigue parameters of various rejuvenator-aged bitumen blends provides the macroscale basis for future nanoscale mechanism exploration and superior rejuvenator development.

1. Introduction

The concept of sustainable development and circular economy is increasingly recognized by infrastructural engineers and researchers [1,2]. Considering the limitation of bitumen resources, it is worth advocating to reuse the waste reclaimed asphalt pavement (RAP) materials during the maintenance and reconstruction of asphalt pavements [3]. As publicly known, the RAP recycling policy greatly benefits cost-reduction, material-saving, and environment-protection [4–6]. However, the RAP involved in asphalt mixture is strictly restricted to low volume because of its high cracking potential and terrible fatigue performance [7,8]. Furthermore, it was reported that incorporating RAP deteriorated the service life of asphalt pavement significantly [9].

The main reason for the short fatigue life of RAP material is the internal aged bitumen with high stiffness and less relaxation capacity [10]. To address this issue, various rejuvenators have been developed to restore the chemo-rheological properties of aged bitumen, and thus its fatigue behavior would be enhanced to some extent [11]. For instance, Cao et al. [12] found that waste vegetable oil could significantly improve the workability and fatigue resistance of aged binders. Similarly, other recycling agents (such as bio oil, paraffinic oil, aromatic extract, tall oil, etc.) exhibited positive effects on prolonging the fatigue life of asphalt binders and mixtures [13].

Nevertheless, the rejuvenation efficiency on fatigue properties is significantly affected by the rejuvenator types and dosages, RAP sources, and percentages [14,15]. Santos et al. [16] mentioned that the bio-oil rejuvenator in aged bitumen showed an excessive mass loss after aging than other rejuvenators, shortening the fatigue life of bio-rejuvenated bitumen. Meanwhile, the conclusions regarding the aging influence on the fatigue life of bitumen from different studies are still inconsistent, resulting from the difference in material characteristics, aging protocol, and fatigue strain level [17]. To develop more high-quality rejuvenators with sufficient rejuvenation effectiveness on fatigue performance recovery, evaluating and comparing the rejuvenation efficiency of different rejuvenator-aged bitumen blends is necessary. Only in this way can we improve the macroscale fatigue performance of rejuvenated bitumen by adjusting rejuvenators' physiochemical characteristics.

* Corresponding author.
E-mail address: Shisong.Ren@tudelft.nl (S. Ren).

https://doi.org/10.1016/j.ijfatigue.2023.107753
Received 8 May 2023; Received in revised form 30 May 2023; Accepted 2 June 2023
Available online 9 June 2023

However, the variations of rejuvenation conditions and characterization tests result in many discrepancies in the literature about rejuvenators' effectiveness in enhancing the fatigue performance of RAP binder and mixture [18,19]. Table 1 lists some cases containing variable material components and fatigue evaluation indices. Until now, various fatigue tests have been adopted to assess the fatigue performance of bitumen blends, including linear viscoelastic measurements, time sweep, linear amplitude sweep, and elastic recovery tests. For each fatigue method, different evaluation indicators are proposed to quantitatively estimate the fatigue property change of bitumen due to aging, rejuvenation, and modification. The Superpave fatigue parameter (G*sinδ), Glover-Rowe (G-R), fatigue failure temperature, rheological index (R), and crossover frequency (ω_c) are used as LVE fatigue indices. Moreover, the TS parameters contain fatigue life N_{f50}, N_{DR}, N_p, N_{p20}, Fatigue damage factor D_R, 50% modulus $G^*_{50\%}$, PA peak, and S × N peak. The viscoelastic continuum damage (VECD) model is always utilized to analyze the LAS results, and different parameters (like A, B, C_1, C_2, α, τ_{max}, $N_{f2.5\%}$, and $N_{f5\%}$) were chosen randomly. Furthermore, the crack width derived from LAS and TS results was also calculated as a fatigue index. It is important and expected to introduce the universal indicators for evaluating the fatigue behavior of rejuvenated binders, considering the influence factors of bitumen components, rejuvenator types/dosages, and aging levels of bitumen.

2. Research limitations and objectives

Based on the literature review, there are still research limitations on the fatigue performance evaluation of rejuvenated bitumen, and some of them are described as follows:

(i) Although most previous studies mentioned that the rejuvenation efficiency of rejuvenator on fatigue performance recovery of aged bitumen significantly depended on the material properties of rejuvenator and aged bitumen, few researchers have comprehensively investigated the effects of these factors on the fatigue performance of rejuvenated binders.
(ii) Different fatigue tests and evaluation parameters were utilized to characterize the fatigue behavior of bituminous materials, but no uniform fatigue test and assessment indicators have been identified, especially when exploring the aging, rejuvenation, and modification influence.
(iii) The diversity of evaluation methods and material components remarkably hinders the mechanism exploration and advanced material development for enhancing the fatigue resistance and self-life of recycled asphalt pavements.

To this end, this study aims to systematically examine the impacts of rejuvenator type/dosage and the aging degree of bitumen on the fatigue performance improvement of aged bitumen. The critical fatigue tests and evaluation indicators on different rejuvenator-aged bitumen blends will be proposed by comparison and screening for future standard formulation. The detailed research methodology is illustrated in Fig. 1. Large sample set will be achieved by preparing different rejuvenated binders with three aging levels, four rejuvenator types, and six rejuvenator dosages. Afterward, three popular fatigue tests (Linear viscoelastic, linear amplitude, and time sweep) will be performed on all fresh/aged/rejuvenated binders to synthetically assess the rejuvenation efficiency of various rejuvenators on the fatigue performance recovery of aged bitumen. For each fatigue test, a series of evaluation parameters will be considered and compared in terms of their sensitivities to variable factors to fully understand the difference in fatigue behaviors of various rejuvenator-aged bitumen systems.

Table 1
Fatigue evaluation indices of various bituminous materials.

Fresh/aged bitumen	Rejuvenator type/ dosage	Fatigue indices	Ref
An extracted RAP binder (Iowa, USA)	Soybean-based rejuvenator with a dosage of 12%	G*sinδ and G-R	[20]
RAP/VG40 blends with R/T = 0.5 and 0.7	Waste vegetable oil with dosages of 5.5% and 11.3%	Failure strain, A, B, C parameters, $N_{f2.5\%}$	[21]
SBS modified bitumen blended with RAP (Yanjin, China)	A rejuvenator with dosages of 2%, 4%, and 6%	Fatigue failure temperature; C_1, C_2, A, B, α, τ_{max}, $N_{f2.5\%}$ and $N_{f5\%}$	[22]
RAP mixture varying from 20 to 40% (Tehran, Iran)	Date seed oil (DSO) with a 5% dosage	G^* and N_f	[23]
Aged bitumen after 20 h and 40 h PAV tests	Aromatic extract and waste cooking-oil with dosage varies from 3.3% to 9.2%	D_f, α, $N_{f2.5\%}$, $N_{f5\%}$, a	[24]
RAP binder (Chongqing, China)	A rejuvenator with 2%, 4%, 6%, and 8% dosages	N_{f50}, N_{DR}, N_p, N_{p20}	[25]
Polymer modified bitumen and fresh bitumen	–	G*sinδ, G-R, ΔTc, A and B	[26]
PG 64–22 base bitumen	Bio-oil with 1%, 3%, and 5% dosages	G*sinδ, R, ω_c, G-R, and N_f	[27]
70# bitumen, short-term aged, and asphalt mastic with 50% mineral powder content	–	D_R and N_f	[28]
PG 58–22 bitumen modified by bio-oil, natural rock, EVA, SBS, and crumb rubber	–	Elastic recovery (ER), $G^*_{50\%}$, PA peak; S × N peak, DER, $N_{f5\%}$, $N_{f10\%}$, $N_{f15\%}$	[29]

Note: ΔTc is the critical temperature of S = 300 MPa and m = 0.3 from bending beam rheometer (BBR); Elastic recovery (ER) is obtained from multiples stress creep and recovery (MSCR) test.

3. Materials and methods

3.1. Materials

Fresh bitumen with a PEN-grade of 70/100 is used to prepare the aged and rejuvenated bitumen. Table 2 displays the chemo-physical properties of fresh bitumen. Meanwhile, four groups of rejuvenators categorized by the National Center for Asphalt Technology (NCAT) [30] in America are involved in this study, including the bio-oil (BO), engine-oil (EO), naphthenic-oil (NO), and aromatic-oil (AO). Their material characteristics are listed in Table 3.

3.2. Preparing aged and rejuvenated bitumen

The fresh bitumen was used to artificially fabricate the aged bitumen using the Thin Film Oven test (TFOT) and Pressure Aging Vessel (PAV) for short-term and long-term aging. For all aged binders, the temperature and aging time of FTOT were 163 ℃ and 5 h. The aging temperature of PAV was 100℃, while the aging time varies from 20 to 40 and 80 h for preparing the aged bitumen with different long-term aging degrees. The fresh and various aging bitumen were abbreviated as VB, LAB20, LAB40, and LAB80.

Twelve groups of rejuvenated bitumen were manufactured with three aging levels and four rejuvenators. The aged bitumen was first preheated and then mixed with rejuvenators at 160 ℃ for 10 mins to ensure homogeneous dispersion of the rejuvenator. Considering the slight aging level, the rejuvenator dosages in LAB20 vary from 1.25% to 10%. To the severely-aged bitumen (LAB40 and LAB80), the rejuvenator concentration changes from 2.5% to 15% with an interval of 2.5%. In total, 72 kinds of rejuvenated binders were fabricated for relaxation behavior characterization considering the coupling effects of

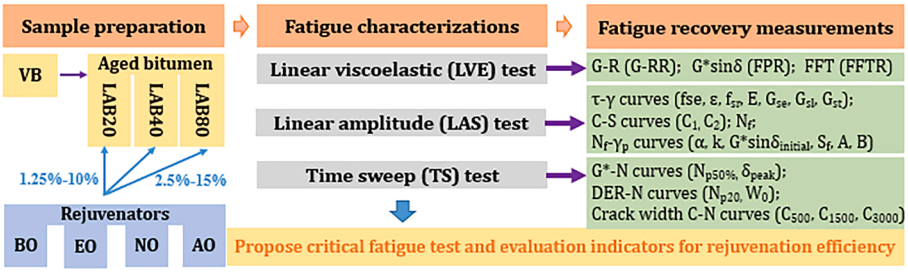

Fig. 1. Research objective and methodology, where G-RR denotes G-R parameter-based rejuvenation percentage; FPR is fatigue parameter-based rejuvenation percentage; FFTR shows fatigue failure temperature-based rejuvenation percentage.

Table 2
Chemo-physical properties of fresh bitumen.

Properties	Value	Specification
25℃ Density /g·cm^{-3}	1.017	EN 15326
25℃ Penetration / 0.1 mm	91	ASTM D35
Softening point / ℃	48.0	ASTM D36
135℃ Viscosity / Pa·s	0.80	AASHTO T316
Saturate dosage / wt%	3.6	
Aromatic dosage / wt%	53.3	ASTM D4121
Resin dosage / wt%	30.3	
Asphaltene dosage / wt%	12.8	

Table 3
Material characteristics of rejuvenators.

Properties	Bio-oil	Engine-oil	Naphthenic-oil	Aromatic-oil
25℃ Density /g·cm^{-3}	0.911	0.833	0.875	0.994
25℃ Viscosity / cP	50	60	130	63,100
Flash point / ℃	265–305	> 225	> 230	> 210
Average weight Mn / g·mol^{-1}	286.43	316.48	357.06	409.99
Carbon dosage / wt%	76.47	85.16	86.24	88.01
Hydrogen dosage / wt%	11.96	14.36	13.62	10.56
Sulfur dosage / wt%	0.06	0.13	0.10	0.48
Oxygen dosage / wt%	11.36	0.12	0.10	0.40
Nitrogen dosage / wt%	0.15	0.23	0.12	0.55

rejuvenator type/dosage and aging grade of bitumen. It should be mentioned that all samples were subjected to both TFOT and PAV tests before performing the fatigue measurements.

3.3. Linear viscoelastic (LVE) measurements

The linear viscoelastic performance of aged and rejuvenated bitumen is assessed using a frequency sweep test with a dynamic shear rheometer (DSR). The diameter and gap between the upper and bottom plates are 8 mm and 2 mm. The frequency rises from 0.01 to 100 rad/s at various testing temperatures of 0, 10, 20, and 40℃. The strain level keeps constant at 0.1% to ensure the LVE response of bitumen. The fatigue parameter G*sinδ is outputted and the value at 10 rad/s is selected to determine the fatigue failure temperature (G*sinδ = 5000 kPa). In addition, the G-R value is calculated following Eq. (1).

$$G-R=\frac{|G^*|(\cos\delta)^2}{\sin\delta} \tag{1}$$

where G* and δ are the complex shear modulus and phase angle at 15 ℃ and 0.005 rad/s.

3.4. Linear amplitude (LAS) test

The LAS tests are performed on all fresh/aged and rejuvenated binders using a DSR device. The graph illustration of applied strain variation and sample dimension of the LAS test is displayed in Fig. 2(a). The diameter and height of the bitumen specimen are 8 mm and 2 mm, respectively. The applied strain increases linearly from 0.1% to 30%. The temperature and frequency are selected as 20℃ and 10 Hz. The total loading cycle number and test time are 3100 cycles and 310 s.

The simplified viscoelastic continuum damage (S-VECD) modelling [31] is adopted to analyze the LAS results. An internal parameter S is introduced to quantify the damaged state of bituminous materials:

$$\frac{ds}{dt}=\left(-\frac{\partial W^R}{\partial S}\right)^{\alpha} \tag{2}$$

where t refers to fatigue time, α shows a material constant related to the rate of damage accumulation, and W^R is the pseudo-strain energy density calculated as follows:

$$W^R=\frac{1}{2}C(S)\left(\gamma^R\right)^2 \tag{3}$$

The C function represents the pseudo stress quantitatively describing material integrity, defined as the ratio of peak stress τ_p and pseudo strain amplitude γ^R. In addition, the γ^R parameter is defined as below:

$$\gamma^R=\frac{(\gamma_p \bullet G^*_{LVE})}{G_R} \tag{4}$$

where γ_p shows the strain amplitude in a fatigue cycle, G_R and G^*_{LVE} are the arbitrary reference modulus and linear viscoelastic shear modulus. Thus, the C function can be rewritten as Eq. (5).

$$C(S)=\frac{\tau_p \bullet G_R}{(\gamma_p \bullet G^*_{LVE})} \tag{5}$$

Meanwhile, the damage state parameter S can be derived as follows:

$$S(t)=\sum_{i=1}^{N}\left[\frac{1}{2}\left(\gamma^R\right)^2(C_{i-1}-C_i)\right]^{\frac{\alpha}{\alpha+1}} \bullet (t_i-t_{i-1})^{\frac{1}{\alpha+1}} \tag{6}$$

where N and i are the load cycles and the cycle number. A power law model is adopted to describe the correlation between the material integrity C and damage parameter S shown in Eq.7. The C_1 and C_2 are the constants.

$$C(S)=1-C_1 \bullet S^{C_2} \tag{7}$$

Based on the above equations, the fatigue life N_f of bituminous material can be predicted from the strain amplitude γ_p using Eq. (8).

$$N_f=\frac{f \bullet 2^{\alpha} \bullet S_f^{1-\alpha C_2+\alpha}}{(1-\alpha C_2+\alpha)(C_1C_2)^{\alpha}\left(\gamma_p \bullet G^*_{LVE}\right)^{2\alpha}} \tag{8}$$

where f refers to the fatigue frequency, and S_f is the damage at a failure point calculated as:

$$S_f=\left(\frac{1-C_f}{C_1}\right)^{\frac{1}{C_2}} \tag{9}$$

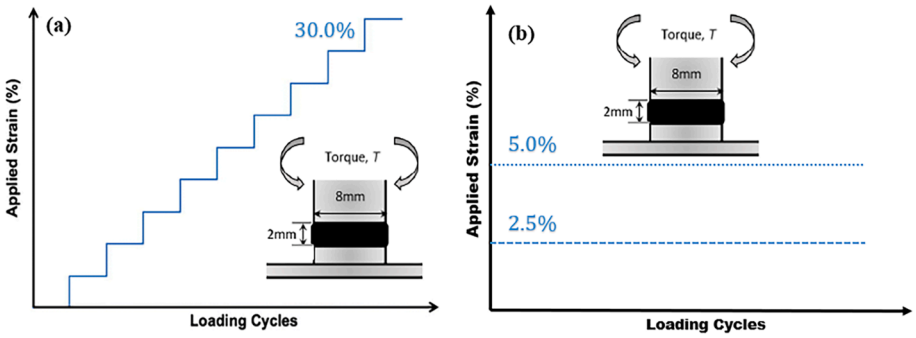

Fig. 2. Fatigue test methods on bituminous materials.

The C_f is the C parameter at the failure point reaching the peak stress. For simplification, the Eq. (8) can be rewritten as follows:

$$N_f = A(\gamma_p)^B \tag{10}$$

where $B = -2\alpha$, and A represents the term displayed in Eq. (11), in which $k = 1 - \alpha C_2 + \alpha$.

$$A = \frac{f \bullet 2^{\alpha} \bullet S_f^k}{k(C_1C_2)^{\alpha}(G^*_{LVE})^{2\alpha}} \tag{11}$$

3.5. Time sweep (TS) test

As shown in Fig. 2(b), 2.5% and 5.0% constant strain levels are applied to perform the TS tests on fresh/aged and rejuvenated bitumen at 20℃. The frequency is 10 Hz, and the DSR specimen size is the same as the LVE test. To ensure data reliability, at least two parallel specimens are measured for all LVE, LAS, and TS tests.

During the fatigue life, three stages of material integrity variation contain (i) No damage; (ii) Crack initiation; and (iii) Crack propagation. The cumulative dissipated energy ratio (DER) can clearly distinguish these three stages, calculated as Eq. (12).

$$DER_n = \frac{\sum_{i=1}^{n} W_i}{W_n} \tag{12}$$

Wi and Wn are the dissipated energies (DE) at the i and n fatigue cycles. And Eq. (13) is used to calculate the DE value.

$$W_i = \pi\tau_{0,i}\gamma_{0,i}\sin(\delta_i) \tag{13}$$

where $\tau_{0,\,I}$ and $\gamma_{0,\,I}$ are the stress and strain amplitudes in the ith cycle.

In the TS test, the variations of shear modulus G* and DER values of bitumen as a function of the loading cycle are detected to measure the fatigue life. The N_{p20} parameter is always used as a failure criterion, defined as the number of loading cycles when the DER value is 20% higher than the corresponding point on the equality line. In addition, the N_{p20} shows an exponential relationship with the initial DE (W_0) values, as displayed in Eq.14.

$$N_{p20} = K_2\left(\frac{1}{W_0}\right)^{K_1} \tag{14}$$

where K_1 and K_2 are the fitting parameters, and it should be noted that the N_{p20} parameter corresponds to the demarcation point between the No damage and Crack initiation stages without considering the Crack propagation part. Table 4 summarizes the test conditions and evaluation indicators of bitumen fatigue performance adopted in this study.

To quantitatively estimate the rejuvenation efficiency of various rejuvenators on the fatigue properties of aged bitumen, a rejuvenation percentage index (PR) is introduced and calculated as follows:

Table 4
Test conditions and evaluation indices of bitumen fatigue performance.

Item	Fatigue tests	Conditions	Parameters
1	LVE test	Frequency sweep at 15 ℃ and 0.005 rad/s	G-R
		Frequency sweep from 10^{-2}-10^{2} rad/s at 0, 10, 20, 30, and 40 ℃	G*sinδ, Fatigue failure temperature
2	LAS test	Linear amplitude sweep at 20℃ and 10 Hz with the strain increasing linearly from 0.1% to 30%	τ-γ curves (f_{se}, ε, f_{sr}, E, G_{se}, G_{sl}, and G_{st}); C-S curves (C_1 and C_2); N_f; N_f-γ_p curves (α, k, $G^*\sin\delta_{initial}$, S_f, A, and B)
3	TS test	Strain-controlled time sweep with 2.5% and 5% strain levels at 20℃ and 10 Hz	G*-N curves ($N_{p50\%}$ and δ_{peak}); DER-N curves (N_{p20} and W_0); Crack width C-N curves (C_{500}, C_{1500}, C_{3000})

$$PR = \frac{P_{aged} - P_{rejuvenated}}{P_{aged} - P_{fresh}} * 100 \tag{15}$$

where PR is the rejuvenation percentage, and P represents the fatigue indices in Table 4. Moreover, the P_{fresh}, P_{aged}, and $P_{rejuvenated}$ are the fatigue indices of fresh, aged, and rejuvenated binders, respectively.

4. Results and discussion

4.1. Linear viscoelastic parameters

4.1.1. G-R parameter

The G-R parameter is an effective index to evaluate bitumen's

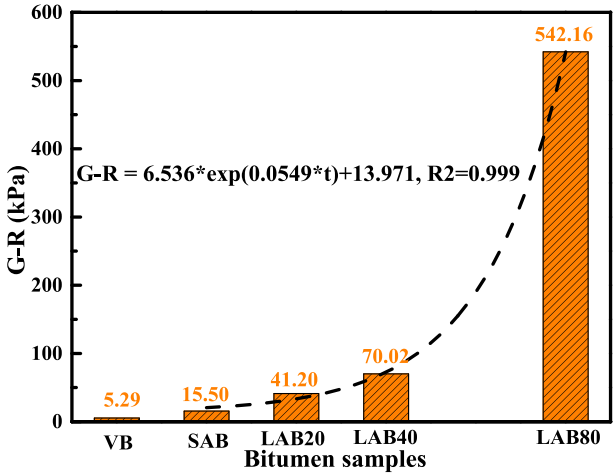

Fig. 3. The variation of the G-R parameter of bitumen.

cohesive ductility and cracking potential. Fig. 3 shows the G-R results of fresh and aged bitumen. The G-R values increase exponentially as the aging degree deepens, especially for the LAB80 binder. Based on the G-R definition shown in Eq.1, the increment in complex modulus G* (stiffness) and decrease of phase angle δ result in the high G-R value of aged bitumen. The exponential correlation formula between the G-R and aging time with a high R^2 value of 0.999 can predict the G-R values of aged binders with other aging levels.

The variation of G-R values of rejuvenated bitumen as a function rejuvenator dosage is shown in Fig. 4. The G-R parameter tends to decrease linearly with the increase in rejuvenator content. The correlation curves between G-R and C values of rejuvenated binders differ significantly due to the difference in rejuvenator type and the aging degree of bitumen. With regard to aging level and rejuvenator dosage, the magnitude of G-R values for rejuvenated bitumen is BORB < EORB < NORB < AORB. It implies that the bio-oil rejuvenated bitumen shows the lowest cracking potential, followed by engine-oil and naphthenic-oil rejuvenated binders, while the aromatic-oil rejuvenated bitumen is most prone to crack. Moreover, the G-R values of all rejuvenated binders increase strongly as the aging degree of bitumen deepens. The absolute slope values in correlation equations of G-R-C curves can reflect the sensitivity of the G-R parameter of rejuvenated bitumen to the rejuvenator content change. It is observed that the sensitivity levels of BORB and AORB are the highest and lowest, which weaken as the aging grade of bitumen increases.

The G-R-based rejuvenation percentages GR-R of all rejuvenator-aged bitumen blends are also presented in Fig. 4. A higher rejuvenator dosage leads to a larger G-RR value of rejuvenated bitumen. An exponential relationship between the G-RR and C parameters is observed for all rejuvenation cases. It indicates that the positive effect of rejuvenator content on G-R recovery of aged bitumen reduces gradually as more rejuvenator is added. The rejuvenator type and aging degree significantly affect the G-RR values and its variation trend versus rejuvenator dosage. The bio-oil and aromatic-oil show the strongest and smallest rejuvenation efficiency on the G-R value of aged bitumen. The engine-oil and naphthenic-oil rejuvenators have similar effects. Meanwhile, a high aging degree of bitumen results in a low rejuvenation efficiency on G-R value. Interestingly, the G-RR values of AORB and NORB binders are much close in LAB80, indicating that aromatic-oil exhibits a significant rejuvenation efficiency in restoring the G-R value of aged bitumen with severe aging degrees.

4.1.2. G*sinδ parameter

The LVE fatigue parameter G*sinδ of fresh and aged bitumen are displayed in Fig. 5 at different temperatures. It is obvious that long-term aging promotes the increase in G*sinδ of bitumen and reduces its temperature sensitivity. High temperatures contribute to the reduction of G*sinδ values of bitumen, and the Log(G*sinδ) exhibits a linear relationship with temperature T. In addition, the Log(G* sinδ) of bitumen shows a linearly increasing trend as the aging level extends. The sensitivity of Log(G* sinδ) to the long-term aging time enlarges as the temperature rises. Thus, the G* sinδ parameter of bitumen is determined by temperature and aging time. The fatigue failure temperatures (FFT) are defined as a temperature when the G*sinδ value equals 5000 kPa, as presented in Fig. 5(c). As the aging time prolongs, the FFT value of bitumen increases exponentially, showing that the fatigue resistance of bitumen strongly deteriorates during the long-term aging time. The molecular mobility and free volume ratio of aged bitumen are much lower than the fresh one, resulting in a worse stress relaxation capacity and cohesion performance [32].

The G*sinδ values and fatigue parameter rejuvenation percentages (FPR) of various rejuvenated binders with variable rejuvenator type/dosage and aging degree of bitumen at 20℃ are illustrated in Fig. 6. The G*sinδ and FPR parameters of all rejuvenated bitumen decrease and increase linearly as a function of rejuvenator dosage. It manifests that all rejuvenators show a rejuvenation effect on restoring the fatigue performance of aged bitumen, but the rejuvenation efficiency strongly relies on the rejuvenator type and aging level of bitumen. The order of G*sinδ values for all rejuvenated binders follows AORB > NORB > EORB > AORB, while the magnitude of FPR is the converse. It suggests that adding bio-oil regenerates the fatigue performance of aged bitumen maximally, followed by engine-oil and naphthenic-oil rejuvenators. In contrast, the rejuvenation efficiency of the aromatic-oil rejuvenator is minimum. The increased aging level reduces the sensitivity of both G*sinδ and FPR to the rejuvenator dosage, enlarges the G*sinδ but decreases the FPR value of rejuvenated binders. It means that the rejuvenation efficiency of rejuvenators on fatigue parameters weakens as the aging degree extends. Further, the ranking of rejuvenation efficiency of four rejuvenators on fatigue parameter is independent of the aging level and rejuvenator content, showing that the G*sinδ is an effective index to quantitatively assess and distinguish the rejuvenation effectiveness of different rejuvenators on the fatigue performance recovery of aged bitumen.

In addition, it should be noted that the rejuvenation percentages of

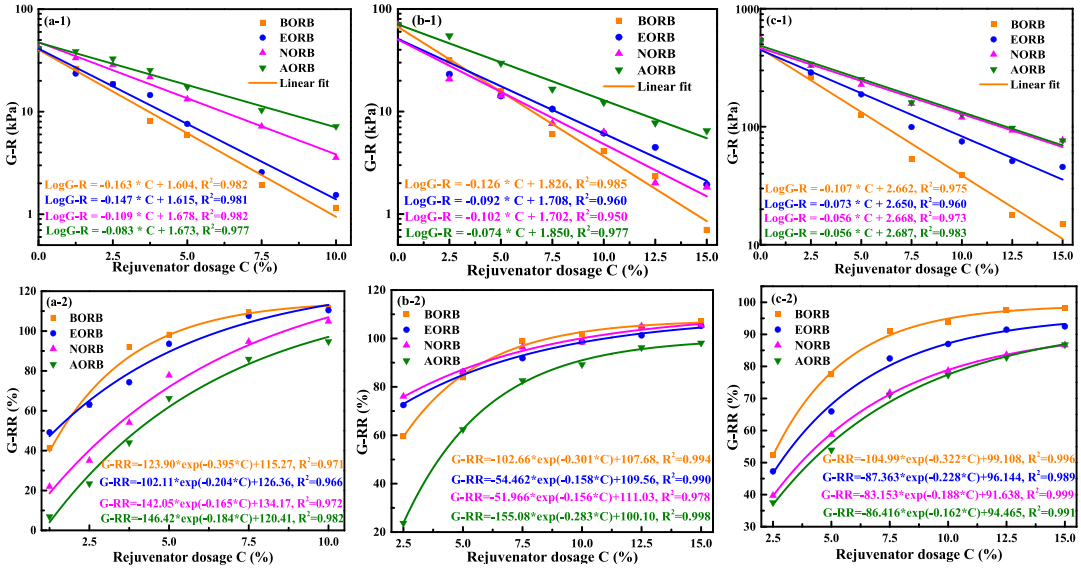

Fig. 4. The G-R values and rejuvenation percentages of rejuvenated bitumen (a-1)(a-2) LAB20; (b-1)(b-2) LAB40; (c-1)(c-2) LAB80.

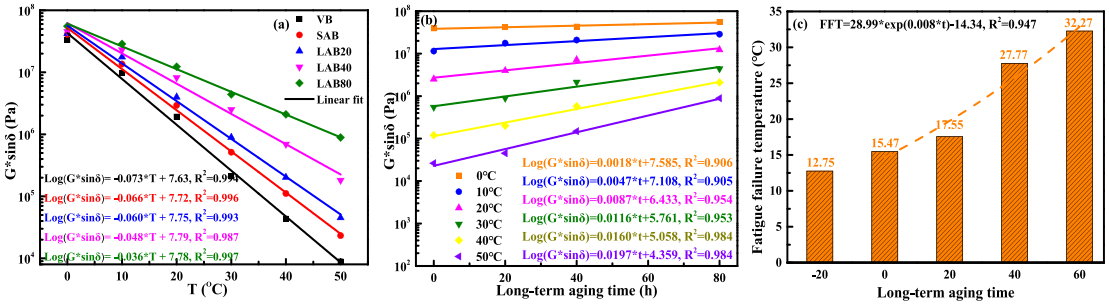

Fig. 5. Aging effect on LVE fatigue characteristics of bitumen.

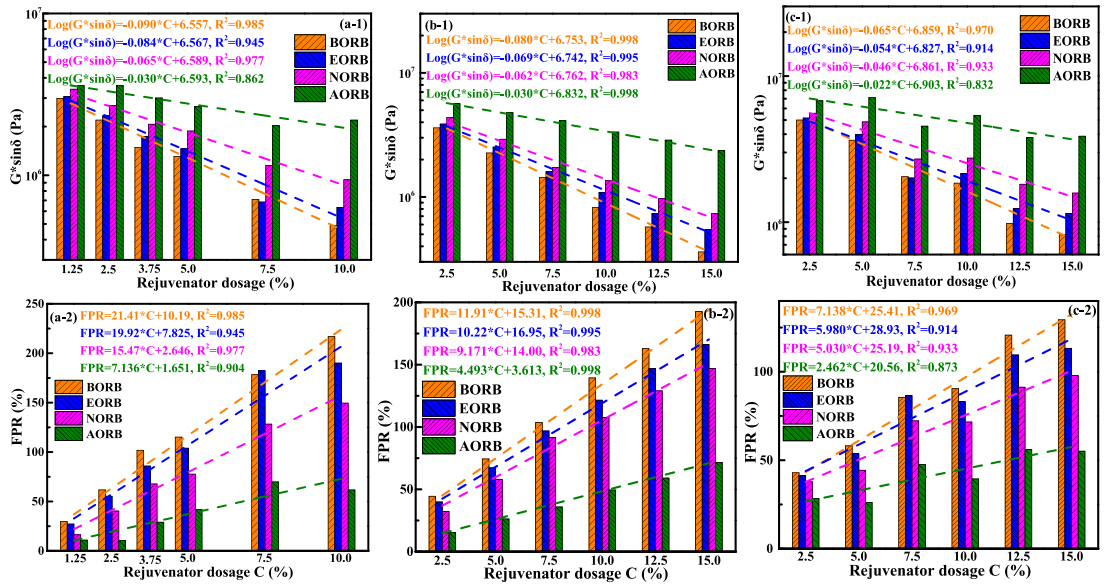

Fig. 6. The G*sinδ values and rejuvenation percentages of rejuvenated bitumen (a-1)(a-2) LAB20; (b-1)(b-2) LAB40; (c-1)(c-2) LAB80.

rejuvenators on the G*sinδ value depend on the test temperatures. Table 5 lists the correlation equation parameters of FPR-C curves at different temperatures of 0, 10, 20, 30, and 40℃. As the temperature rises, the FPR values of rejuvenated bitumen gradually decrease, but the reduction trend is not significant when the temperature is higher than 30℃. It means that the rejuvenation efficiency of rejuvenators on G*sinδ restoration of aged bitumen tends to decrease at high temperatures. Meanwhile, the variation rate of FPR value to rejuvenator dosage significantly reduces with the increase of temperature and aging degree, which shows no effect on the ranking of FPR values for four rejuvenators (BO > EO > NO > AO).

4.1.3. Fatigue failure temperature (FFT)

The FFT parameter of bitumen is determined based on the G*sinδ-T curves and the critical G*sinδ value of 5000 kPa related to the cracking potential. The FFT values and corresponding rejuvenation percentages FFTR of all rejuvenator-aged bitumen blends are drawn in Fig. 7. The linear variation law of FFT and FFTR to the rejuvenator dosage is similar to the Log(G*sinδ) and FPR parameters, respectively. It should be mentioned that the bitumen with a lower FFT value would behave with a greater fatigue resistance. Regardless of rejuvenator dosage and aging grade, the ranking of FFT values of rejuvenated binders is AORB > NORB > EORB > BORB, and the FFTR shows the opposite trend. Similar to the G*sinδ, the roles of rejuvenator type/dosage and aging degree of bitumen in affecting the rejuvenation efficiency on the fatigue performance can be recognized with the FFT index. Although the G-R value of aged bitumen can be restored by adding rejuvenators, the magnitude of G-RR for four rejuvenators varies greatly versus the rejuvenator content and aging degree of bitumen. Thus, the G-R fails to be a critical LVE index for rejuvenation efficiency evaluation on fatigue property. The G*sinδ and FFT parameters meet the requirement, but choose one of them because of high similarity. Due to the temperature independence, the FFT is recommended as the evaluation index for the LVE fatigue performance of various rejuvenator-aged bitumen systems.

4.2. LAS test parameters

4.2.1. Linear viscoelastic response

The LVE G* region of undamaged bitumen must be measured before performing the LAS tests. The fresh/aged and rejuvenated bitumen results are plotted in Figs. 8 and 9, respectively. As the frequency increases, the complex modulus G* of all binders enlarges distinctly, and there is a linear correlation between the Log(G*) values and frequency. The long-term aging promotes the increment in G* value (especially at low-frequency regions) but reduces its sensitivity level to the frequency. With the rejuvenator dosage rising, the G* value of rejuvenated bitumen decreases, and its frequency sensitivity enlarges.

Interestingly, the G* value of aged bitumen can be recovered, but the sensitivity levels of all LAB40 rejuvenated binders to the frequency are lower than the fresh bitumen. It is mainly related to the limited restoration of these rejuvenators on the colloidal structure of bitumen. The magnitude of G* values of rejuvenated binders is BORB < EORB < NORB < AORB, indicating that the bio-oil and aromatic-oil show the best and worst softening effect on the stiffness of aged bitumen, respectively. Generally, the bio-oil rejuvenator has the highest rejuvenation effect on the frequency dependence of the G* parameter.

Table 5
FPR-C correlation equations of rejuvenated binders.

Aging level	T (℃)	Samples	k	b	R^2	Samples	k	b	R^2
	0		45.74	61.75	0.992		32.48	55.10	0.983
	10		24.41	39.83	0.990		17.62	33.09	0.982
	20	BORB	21.41	10.19	0.985	NORB	15.47	2.65	0.977
	30		12.11	10.28	0.987		8.80	5.17	0.972
LAB20	40		11.02	9.03	0.985		7.91	6.39	0.975
	0		45.68	63.79	0.955		10.97	25.10	0.954
	10		23.16	39.16	0.956		6.74	25.31	0.907
	20	EORB	19.92	7.83	0.946	AORB	7.14	1.65	0.924
	30		11.15	6.42	0.965		5.46	1.42	0.996
	40		9.73	8.02	0.952		5.09	2.94	0.953
	0		41.10	12.30	0.994		29.81	37.50	0.982
	10		18.45	20.09	0.996		13.88	22.53	0.982
	20	BORB	11.91	15.31	0.998	NORB	9.17	14.00	0.983
	30		7.09	17.81	0.982		5.42	16.97	0.998
LAB40	40		6.09	17.67	0.985		4.91	16.43	0.996
	0		36.56	28.26	0.998		4.59	20.21	0.957
	10		16.29	22.37	0.997		4.42	11.35	0.996
	20	EORB	10.22	16.95	0.995	AORB	4.49	3.61	0.998
	30		6.19	16.02	0.990		3.45	7.28	0.999
	40		5.31	16.21	0.993		3.60	7.86	0.994
	0		19.26	56.11	0.985		13.71	63.21	0.958
	10		11.11	34.71	0.980		8.01	35.31	0.954
	20	BORB	7.14	25.41	0.970	NORB	5.03	25.19	0.933
	30		4.87	19.46	0.971		3.43	18.95	0.924
LAB80	40		3.78	26.19	0.959		2.75	24.83	0.923
	0		17.18	70.87	0.958		4.87	22.96	0.936
	10		9.51	41.62	0.938		2.67	26.65	0.897
	20	EORB	5.98	28.93	0.914	AORB	2.46	20.56	0.931
	30		3.95	21.73	0.939		2.27	15.55	0.907
	40		3.07	27.44	0.931		2.19	23.11	0.916

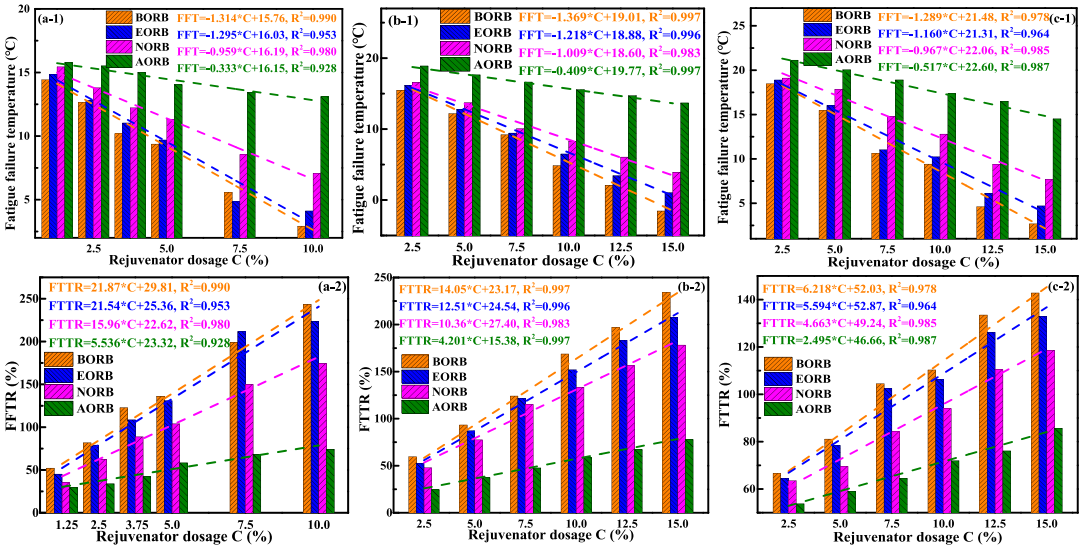

Fig. 7. The FFT and FFTR values of rejuvenated bitumen (a-1)(a-2) LAB20; (b-1)(b-2) LAB40; (c-1)(c-2) LAB80.

However, when the AORB with high aromatic-oil content (12.5% and 15%) shows the most heightened sensitivity of G* values to frequency, which may be attributed to its positive effect on the deagglomeration of polar molecules (resin and asphaltene clusters) in aged bitumen.

4.2.2. Shear stress–strain curves and derived parameters

The shear stress–strain curves of fresh and aged bitumen during the LAS tests are shown in Fig. 10(a). As the shear strain rises from 0.1% to 30%, the corresponding stress increases to a maximum point and decreases gradually. Long-term aging significantly affects the stress–strain response of bitumen. As the aging degree extends, the stress–strain curve of bitumen becomes narrower and taller. The increased maximum stress of bitumen is associated with the high stiffness of aged bitumen, and a high aging degree promotes the strain sensitivity of the shear stress. Although the peak value of bitumen stress is enhanced, a high aging degree accelerates the fatigue damage of bitumen. To quantitatively reflect the effects of aging and rejuvenation on the stress–strain response of bitumen, the stress–strain curve is divided into three pieces: the elastic stage, the stress accumulation stage, and the localized cracking [33], which are illustrated in Fig. 10(b). These evaluation indices derived from the strain–stress curve are the f_{se}, f_{sr}, ε_{se}, ε_{sr}, E, G_{se}, G_{ss}, and G_{sl}. The f_{se} and ε_{se} are the maximum elastic stress and strain in the elastic stage, and the E parameter refers to the elastic modulus ($E = f_{se}/\varepsilon_{se}$). Moreover, the f_{sr} and ε_{sr} represent the peak stress and strain. The

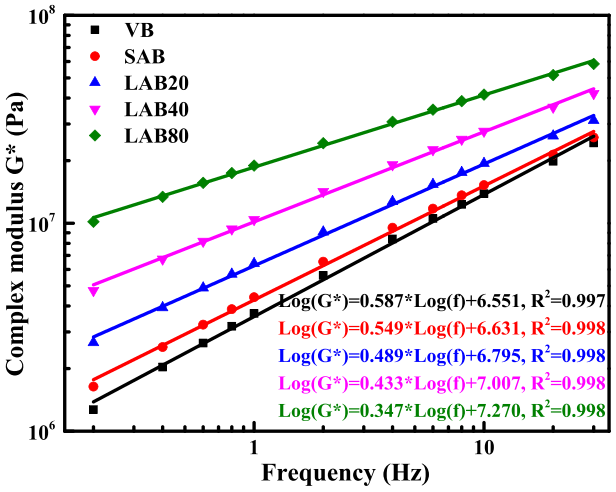

Fig. 8. Frequency sweep curves of fresh and aged bitumen.

fracture energies at different stages are derived as follows:

$$G_{se} = \int_0^{\varepsilon_{se}} f(\varepsilon)d\varepsilon$$

$$G_{ss} = \int_{\varepsilon_{se}}^{\varepsilon_{sr}} f(\varepsilon)d\varepsilon \quad (16)$$

$$G_{sl} = \int_{\varepsilon_{sr}}^{\varepsilon_{st}} f(\varepsilon)d\varepsilon$$

The effects of long-term aging time on the stress–strain curve parameters of bitumen are shown in Fig. 11. Linear relationships between the aging time with these parameters are observed, which can be utilized to predict the stress–strain curves of aged bitumen with various aging degrees. As the aging level deepens, the Log(f_{se}) and Log(f_{sr}) values tend to increase linearly, and the f_{se} parameter shows greater sensitivity to the aging time. The ε_{se} of all fresh and aged bitumen are similar, but the ε_{sr} value reduces linearly as the aging time extends. It indicates that long-term aging does not influence the elastic region but weakens the bitumen's stress accumulation capacity. Moreover, the elastic modulus E of bitumen significantly enlarges due to the increased aging level. The stronger intermolecular interactions and lower free volume between bitumen molecules reflect higher shear stress and modulus at a fixed

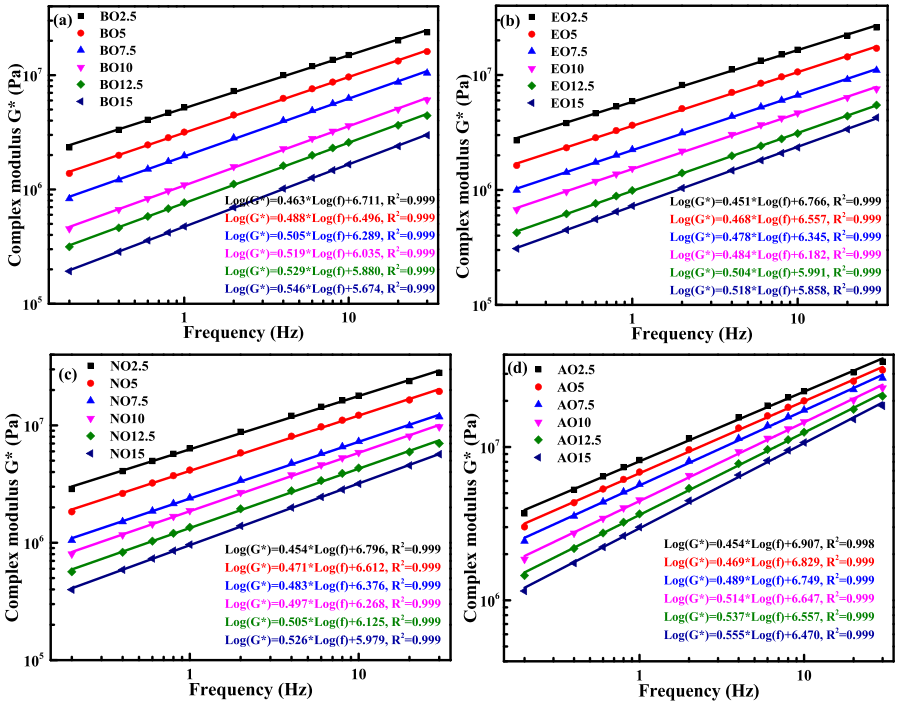

Fig. 9. Frequency sweep curves of LAB40 rejuvenated bitumen.

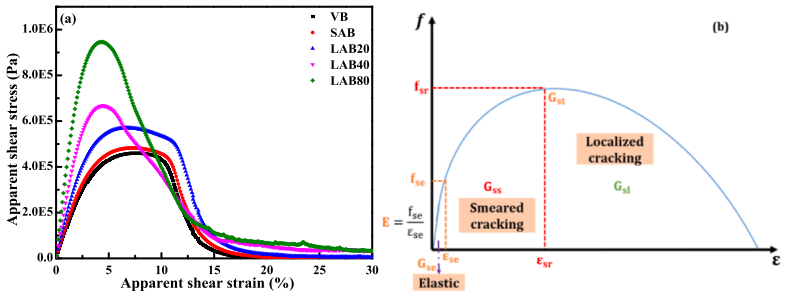

Fig. 10. The stress–strain (f-ε) curves of fresh/aged bitumen (a) and evaluation indicators (b).

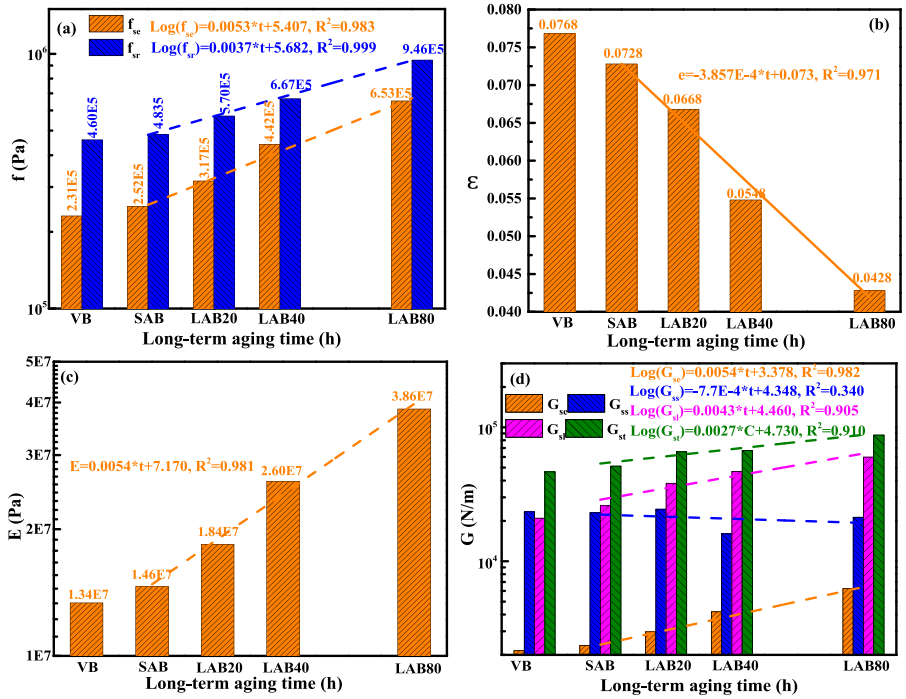

Fig. 11. Effects of long-term aging on stress–strain curve parameters.

strain level. Further, the fracture energies G_{se} and G_{sl} of bitumen show a distinct increasing trend with the aging time prolonging, but the G_{ss} value decreases linearly. It suggests that long-term aging improves the elastic performance and local fracture energy but shortens the cracking time. Due to the low sensitivity of ε_{se} and G_{ss} to aging, these two parameters will not be considered while evaluating the rejuvenation effects on the stress–strain curve of aged bitumen.

The stress–strain curves of LAB40 rejuvenated binders are displayed in Fig. 12. For all rejuvenators, as the rejuvenator dosage rises from 2.5% to 15%, the stress–strain curves of rejuvenated bitumen transfer to the bottom-right direct, which is opposite to the aging effect. It manifests that incorporating rejuvenators can significantly restore the stress–strain response of aged bitumen to fresh one. It is found that the f_{sr} value decreases, but the ε_{sr} increases distinctly when more rejuvenator is added. However, various rejuvenators exhibit different restoration effects on a stress–strain curve when the rejuvenator concentration is fixed. The stress–strain curves of aromatic-oil rejuvenated binders are the steepest, indicating that the aromatic-oil rejuvenator shows the lowest rejuvenation effect on the stress–strain response of aged bitumen. Meanwhile, the f_{sr} and ε_{sr} values of bio-oil and engine-oil rejuvenated

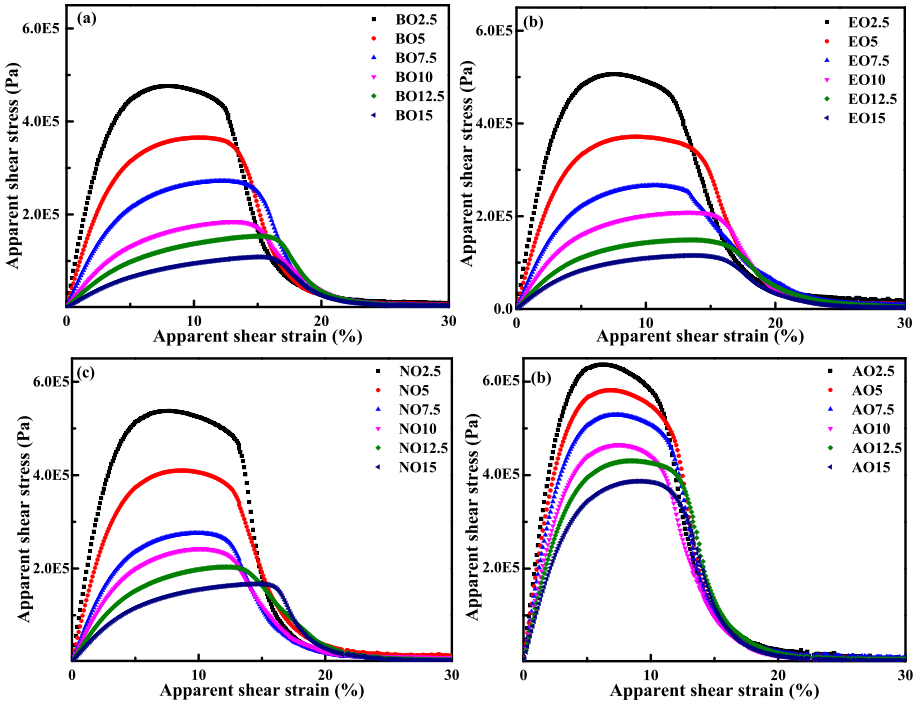

Fig. 12. The shear stress–strain curves of LAB40 rejuvenated bitumen.

bitumen are lower and larger than that of naphthenic-oil rejuvenated bitumen. Interestingly, the positive impact of rejuvenator dosage on stress–strain curves is more noticeable at low concertation (2.5% to 7.5%) for BORB, EORB, and AORB binders. Nevertheless, the difference in the change rate of stress–strain curves of AORB binders with different AO contents is not obvious. In addition, the f_{sr} and ε_{sr} of AO15 bitumen are higher and lower than that of BO5, EO5, and NO7.5 binders. It implies that the aromatic-oil rejuvenated bitumen shows more cracking potential than the others due to the limited number of lightweight molecules in aromatic-oil [34].

The stress–strain curve parameters and corresponding rejuvenation percentages of various LAB40 rejuvenated bitumen are plotted in Fig. 13. As the rejuvenator dosage rises, the logarithmic values of f_{se}, f_{sr}, E, G_{se}, and G_{sl} of rejuvenated bitumen decrease linearly, whereas the E parameter tends to increase linearly. These parameters of rejuvenated binders with different rejuvenator types/dosages can be predicted with the correlation equations also presented in Fig. 13. Meanwhile, these stress–strain response parameters of rejuvenated bitumen strongly depend on the rejuvenator type. For parameters f_{se}, f_{sr}, E, G_{se}, and G_{sl}, the magnitude of rejuvenated binders is the same as AORB > NORB > EORB > BORB, while the order of E value shows the opposite trend. However, some parameters of different rejuvenated binders are hard to distinguish, such as the f_{sr} and G_{se} values of BORB and EORB, and the G_{sl} parameter of EORB and NORB binders. Thus, these parameters are improper in classifying the rejuvenation efficiency of various rejuvenators on the stress–strain response of aged bitumen. Moreover, a rejuvenator exhibits different rejuvenation influences on these stress–-strain parameters. Therefore, it is necessary to specify and simplify the evaluation parameters when the rejuvenation efficiency of rejuvenators on fatigue behaviors is investigated.

In addition, stress–strain parameters-based rejuvenation percentages show a linear increasing trend as the rejuvenator content increases. It indicates that these four rejuvenators can restore all aged bitumen stress–strain curve parameters, but the rejuvenator and evaluation index types affect the rejuvenation efficiency. The bio-oil and aromatic-oil rejuvenated binders exhibit the largest and smallest rejuvenation percentages. Meanwhile, the engine-oil and naphthenic-oil show moderate rejuvenation efficiency, which is much better than the aromatic-oil. However, some overlap sections in the f_{sr}R-C and G_{se}R-C curves of BORB and EORB at high rejuvenator dosages and the G_{sl}R-C curves of EORB and NORB are observed. Therefore, these parameters are not the first choice for evaluating and distinguishing the rejuvenation efficiency

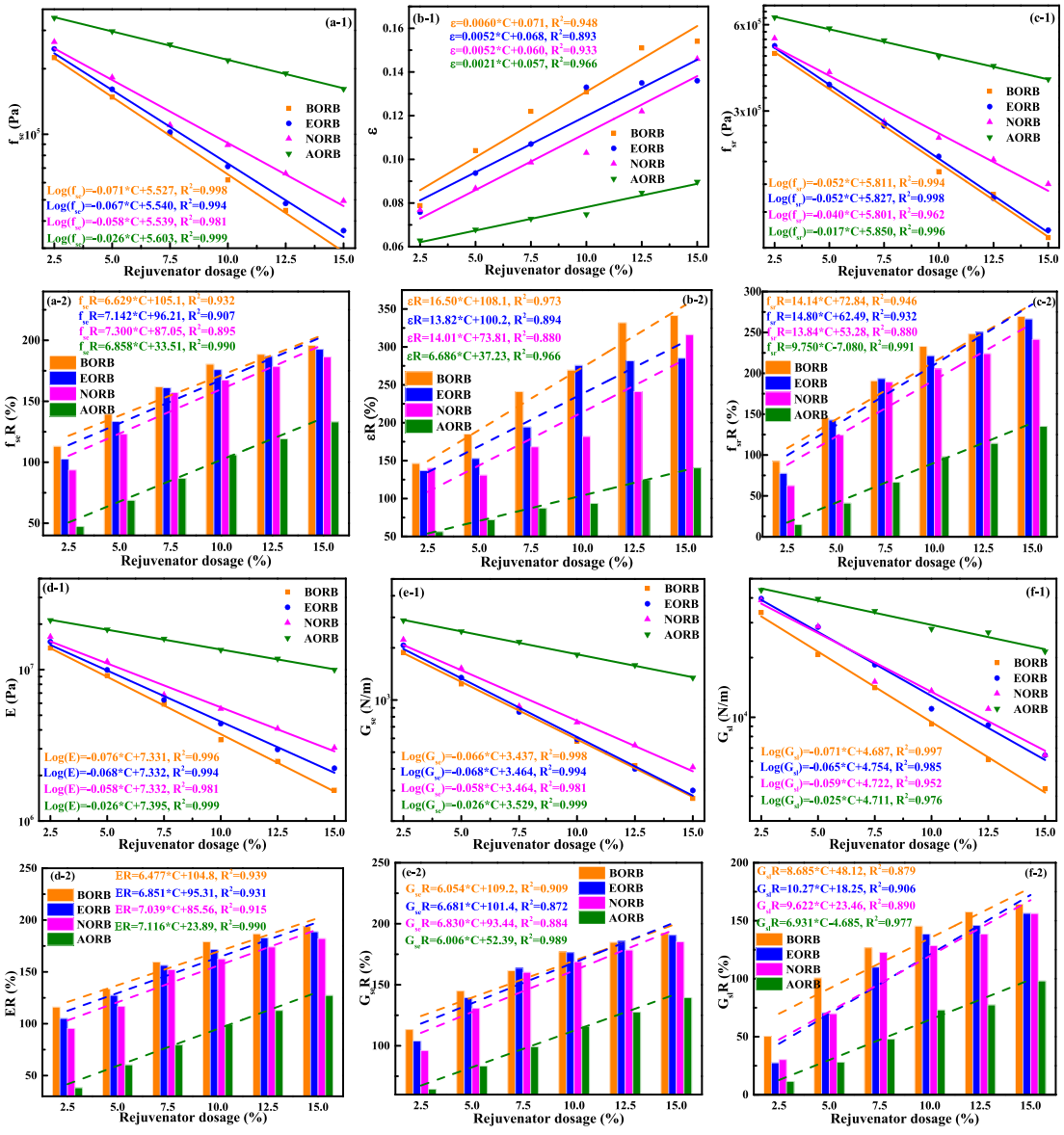

Fig. 13. Rejuvenation effect on strain–stress parameters of aged bitumen.

of various rejuvenators on the stress–strain response. Conversely, the f_{se}, ε_{sr}, and E parameters work well. It should be noticed that rejuvenators have different rejuvenation percentages on these parameters. The percentage regions for f_{se}, ε_{sr}, f_{sr}, E, G_{se}, and G_{sl} of all rejuvenator-aged bitumen blends are 0–310%, 0–600%, 0–400%, 0–320%, 0–300%, and 0–200%, respectively. The ε_{sr}R scope is much wider than the others, and the f_{se}R and ER ranges are similar to the other parameters. Overall, the ε_{sr}, f_{se}, and E parameters derived from the stress–strain curves can effectively evaluate the rejuvenation efficiency of various rejuvenators on the fracture potential of all rejuvenator-aged bitumen systems.

4.2.3. C-S curves and derived parameters

The C-S curves can directly reflect the material characteristic variation during the fatigue damage. Based on **Eq. (7)**, the material integrity C of bitumen shows an exponential relationship with the damage intensity S. The changes of constants C_1 and C_2 can be detected to quantitively evaluate the aging and rejuvenation effects on the C-S curves of bitumen. Fig. 14(a) presents the C-S curves and correlation formulas of fresh and aged bitumen. As the damage intensity S rises, the C value decreases gradually. A high aging degree accelerates the reduction trend of the C parameter. It shows that the deterioration level of bitumen intensifies as the long-term aging time prolongs. The influence of aging on the constants C_1 and C_2 of C-S curves is depicted in Fig. 14(b). As the aging time extends, the C_1 value rises, but the C_2 parameter declines linearly. It implies that a high aging degree intensifies the deterioration rate of material integrity but relieves its sensitivity to the damage intensity S of bitumen. This phenomenon is also observed in strain–stress curves, which reveal that the aging degree enlarges the destruction threshold but promotes the damage rate.

Fig. 15 depicts C-S curves of LAB40 rejuvenated bitumen with variable rejuvenator types and dosages. Increasing rejuvenator content leads to the C-S curves of rejuvenated bitumen moving to the upper right for all rejuvenated binders. These rejuvenators can renovate the C-S curve of aged bitumen to the fresh bitumen level. When the damage intensity S keeps constant, the C parameter of rejuvenated bitumen improves significantly as the rejuvenator dosage rises, and thus the corresponding fatigue life will extend. Moreover, the rejuvenator type greatly influences the restoration effectiveness of C-S curves. Adding bio-oil recovers the C-S curves to the greatest extent, followed by the engine-oil and naphthenic-oil, while the aromatic-oil shows the lowest rejuvenation effect.

Fig. 16 displays the C_1, C_2 values and their rejuvenation percentages (C_1R and C_2R) of rejuvenated bitumen, showing linear relationships with the rejuvenator dosage. C_1 and C_2 correlate negatively and positively with increased rejuvenator content. This variation trend is the opposite of the aging case, indicating that the inclusion of rejuvenators dramatically improves the C-S response of aged bitumen. The rejuvenation efficiency of various rejuvenators on C_1 and C_2 parameters are different. In detail, the magnitude of C_1R values is BORB > NORB > EORB > AORB, while the order of the C_2R parameter follows BORB > AORB > NORB > EORB. Therefore, neither one can fully reflect the rejuvenation efficiency of different rejuvenators on the C-S curve of aged bitumen.

4.2.4. Fatigue life N_f and rejuvenation percentage

The N_f and N_fR values are calculated using Eqs. (8) and (15), respectively. The fresh and aged bitumen results are shown in Fig. 17. The relationship between the N_f of bitumen and strain level agrees well with Eq.10, and the Log(N_f) value decreases linearly as the logarithmic value of shear strain increases. It is interesting to notice that there is no consistent influence law of long-term aging time on the N_f values of bitumen in the entire strain region. At low strains (1%–2%), the N_f value of bitumen tends to increase as the aging level deepens, which presents an opposite trend when strain is higher than 4%. Based on the correlation equations, the aging degree promotes the enlargement in the initial N_f value of bitumen, increasing the reduction rate of the N_f parameter to the strain level. To keep consistent with the following sweep (TS) test, the N_f parameters at two strain levels of 2.5% and 5% are considered to assess the fatigue life of bitumen with different aging and rejuvenation conditions. To the N_f parameter at 2.5% strain ($N_{f2.5}$), the short-term aging shows a positive effect, slightly reducing after 20 h long-term aging. However, the $N_{f2.5}$ values of LAB40 and LAB80 continue to rise, even larger than the fresh bitumen.

Thus, the evaluation result regarding the aging effect on the fatigue life of bitumen significantly depends on the applied strain level. In addition, the N_f value of bitumen at 5% strain (N_{f5}) declines exponentially as the aging time prolongs. The N_{f5} of aged binders with different aging levels longer than LAB80 can be predicted using the N_f-t relational formula. Fig. 18 displays the N_f and N_fR values at 2.5% and 5% strains of LAB40 rejuvenated bitumen. Regardless of strain level, the N_f values of rejuvenated binders increase linearly as the rejuvenator dosage rises. It suggests that incorporating rejuvenators improves fatigue resistance and extends the service life of aged bitumen. As expected, the N_{f5} values are lower than the $N_{f2.5}$. The apparent difference in the enhancement level of four rejuvenators on the N_f of aged bitumen shows BORB > EORB > NORB > AORB. It further signifies that the bio-oil maximally enhances the fatigue life of aged bitumen, followed by engine-oil and naphthenic-oil, while the aromatic-oil has the lowest fatigue life extension capacity. It should be mentioned that the difference in N_f values of rejuvenated binders with various rejuvenators is significant, indicating that the N_f is an effective indicator to evaluate and discriminate the fatigue life of different rejuvenator-aged bitumen blends.

As the rejuvenator dosage increases, the N_fR_5 increases linearly, but the $N_fR_{2.5}$ shows a linearly decreasing trend. The reason for the negative $N_fR_{2.5}$ values is that the N_f of aged bitumen at 2.5% strain is higher than the fresh bitumen, and the inclusion of rejuvenators continues to enlarge the $N_{f2.5}$ value of aged bitumen. Therefore, the $N_{f2.5}$ results violate the rejuvenation definition and fail to assess the rejuvenation efficiency of rejuvenators on the fatigue performance of aged bitumen. On the contrary, the N_fR_5 values can effectively and quantitatively estimate the

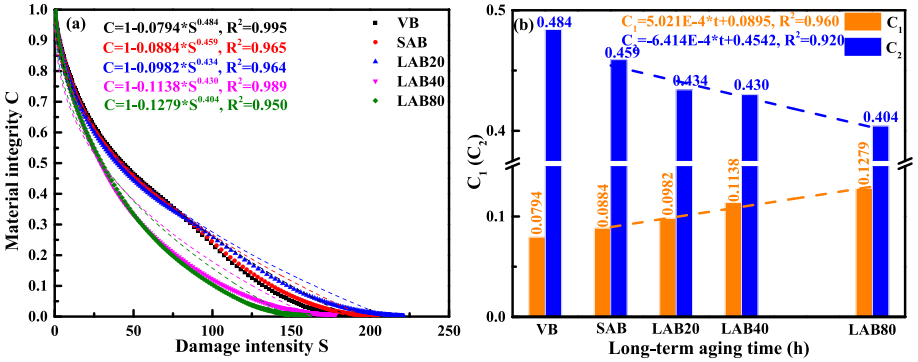

Fig. 14. Aging effect on C-S curves and model parameters.

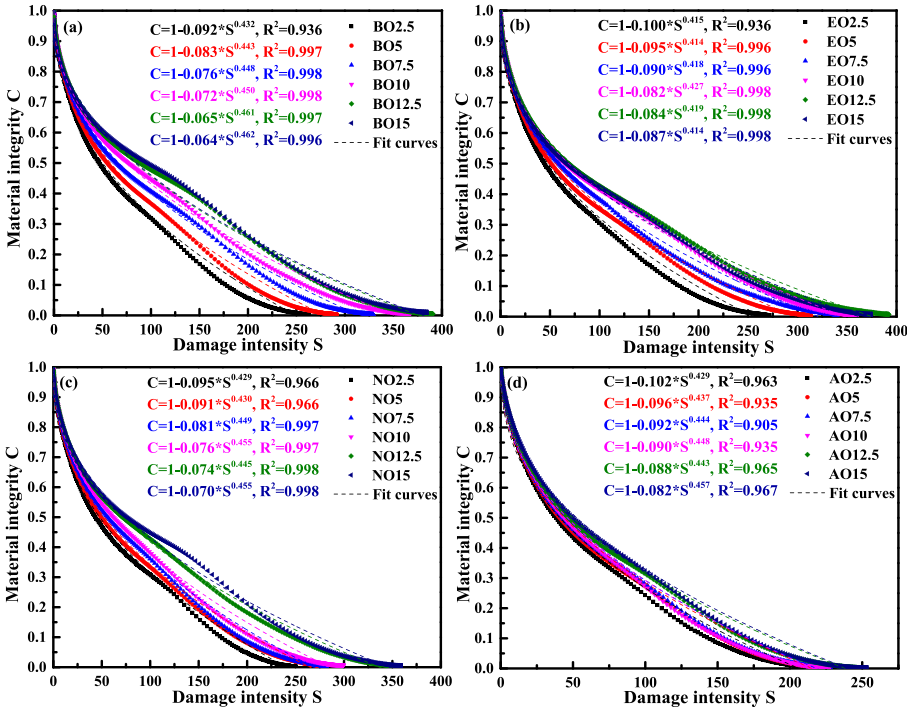

Fig. 15. The C-S curves of various rejuvenated bitumen.

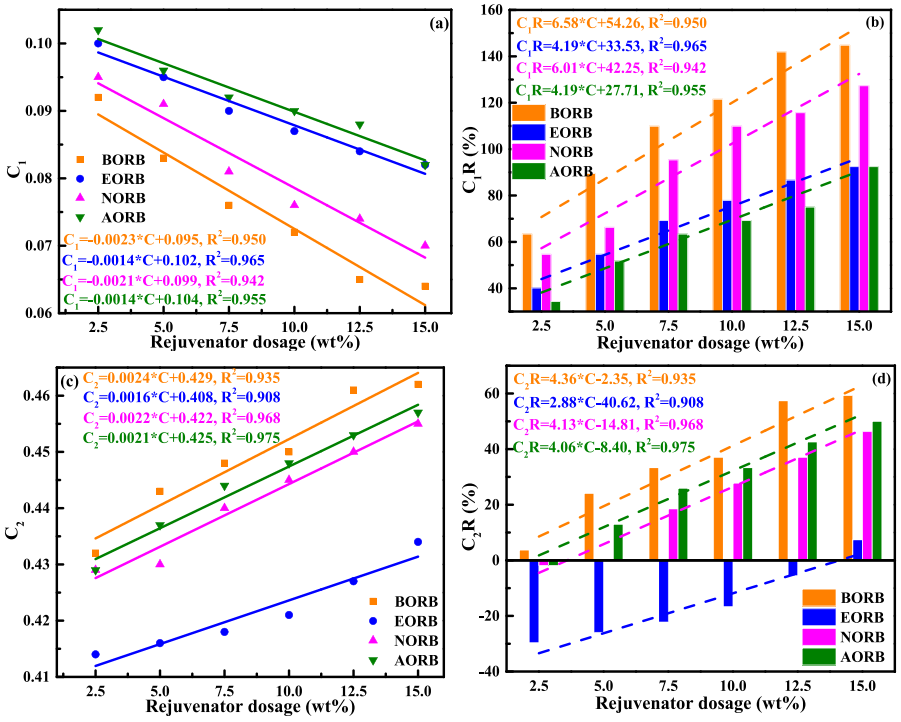

Fig. 16. The rejuvenation effect on C-S curve model parameters.

rejuvenation efficiency of various rejuvenators on fatigue life, and the scope of N_fR_5 values (0–550%) is much wider than the stress–strain curve and C-S curve parameters. Table 6 lists the correlation equations of N_f-C and N_fR-C curves of rejuvenated binders with variable aging degrees. The fatigue life and corresponding rejuvenation percentage.

are remarkably influenced by the aging level of bitumen. When the strain level is 2.5%, the high aging degree enlarges the $N_{f2.5}$ values of rejuvenated bitumen. The $N_fR_{2.5}$ values of LAB20 rejuvenated are positive, which becomes negative for both LAB40 and LAB80 cases. The aging level effect is more significant regarding the Nf5 and NfR5 values. The severe aging degree of bitumen reduces the fatigue life and rejuvenation percentages of rejuvenators when the rejuvenator type/dosage is the same. Furthermore, the ranking of N_{f5} and N_fR_5 is invariable as BORB > EORB > NORB > AORB.

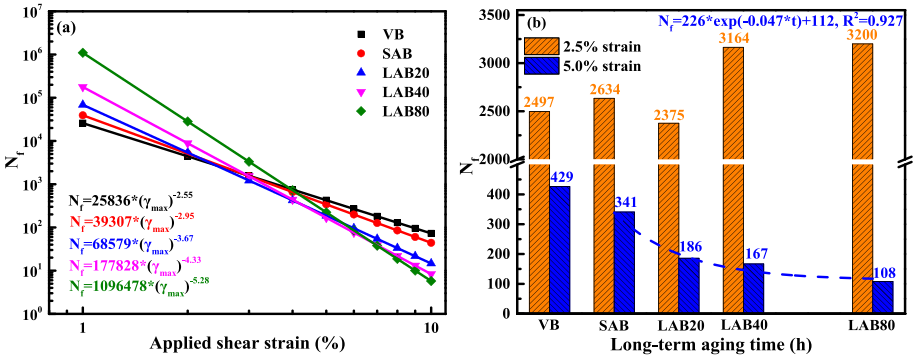

Fig. 17. Influence of long-term aging on N_f values of bitumen.

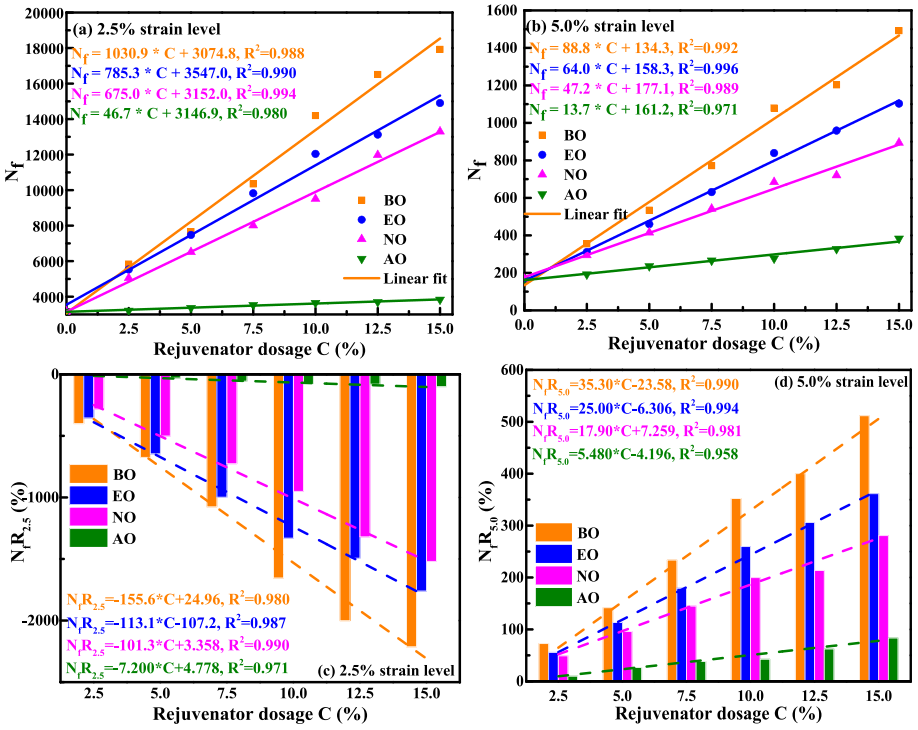

Fig. 18. N_f and N_fR values of LAB40 rejuvenated bitumen.

4.2.5. LAS curve fitting parameters

It has been proved that the rejuvenation efficiency strongly relies on the evaluation parameters. The LAS results analysis introduces various parameters in Eqs.8–11, including the α, k, G*sinδ$_{initial}$, S_f, A, and B. The influence of aging and rejuvenation on fatigue performance from LAS tests is a joint result of their effects on these parameters. This section aims to investigate these parameters' variation of bitumen due to different aging and rejuvenation conditions and propose several critical evaluation indicators reflecting the rejuvenation efficiency of various rejuvenator-aged bitumen blends. The results of fresh and aged bitumen are shown in Fig. 19. The parameters α, k, and G*sinδ$_{initial}$ increase linearly as the aging time prolongs. By definition, parameter α refers to the rate of damage accumulation, and a high aging level promotes the deterioration rate of bitumen. The k is derived from the parameters α and C_2, which increases and reduces as the aging degree deepens. It results in a positive correlation between the k and aging time t. The aging time dependence of the k parameter is determined by the variation rate of α and C_2, and the former is much larger than the latter. Thus, the k parameter shows less sensitivity to the aging time than the α. Similar to the fatigue parameter discussed in section 4.1.2, the G*sinδ$_{initial}$ value of bitumen enlarges significantly during the long-term aging process, indicating that the fatigue resistance of bitumen weakens gradually. The S_f parameter is the damage intensity at the fatigue failure point, which decreases exponentially due to increased aging time. It means that a high aging degree leads to an earlier break point of bitumen. By definition (B = -2α), the B parameter presents an opposite trend to the α with a two times variation rate versus aging time. Further, the A parameter is determined by different terms, and the aging time promotes its exponential increment, especially when the aging level deepens from LAB40 to LAB80.

Fig. 20 depicts the LAS parameters and corresponding rejuvenation percentages of rejuvenated bitumen, considering the influence of rejuvenator type and dosage. All LAS parameters and their rejuvenation percentages show linear correlations with rejuvenator content. In detail, the α, k, and G*sinδ$_{initial}$ values of rejuvenated bitumen decrease as the rejuvenator dosage increases, while the S_f, A, and B parameters enlarge. Compared with the aging effect, these rejuvenators can restore most LAS parameters of aged bitumen toward fresh level, except the parameter A determined by all the rest LAS parameters as Eq.11. That's why the negative AR values of BORB, EORB, and NORB binders are observed. However, the aromatic-oil rejuvenator can restore the A parameter, but the rejuvenation effectiveness is limited. Thus, parameter A is excluded

Table 6
Correlation equations of N_f-C and N_fR-C curves.

	Samples	LAB20	LAB40	LAB80
$N_{f2.5}$	BORB	$N_{f2.5} = 694.2*C + 2460.9$	$N_{f2.5} = 1030.9*C + 3074.8$	$N_{f2.5} = 1072.3*C + 3306.3$
	EORB	$N_{f2.5} = 656.5*C + 2209.3$	$N_{f2.5} = 785.3*C + 3547.0$	$N_{f2.5} = 903.6*C + 3226.8$
	NORB	$N_{f2.5} = 625.8*C + 2349.3$	$N_{f2.5} = 675.0*C + 3152.0$	$N_{f2.5} = 737.6*C + 3597.8$
	AORB	$N_{f2.5} = 81.1*C + 2380.9$	$N_{f2.5} = 46.7*C + 3146.9$	$N_{f2.5} = 70.0*C + 3172.5$
$N_fR_{2.5}$	BORB	$N_fR_{2.5} = 562.4*C + 115.3$	$N_fR_{2.5} = -155.6*C + 24.96$	$N_fR_{2.5} = -151.3*C-28.22$
	EORB	$N_fR_{2.5} = 550.9*C-222.3$	$N_fR_{2.5} = -113.1*C-107.2$	$N_fR_{2.5} = -128.2*C-7.122$
	NORB	$N_fR_{2.5} = 514.9*C-34.47$	$N_fR_{2.5} = -101.3*C + 3.358$	$N_fR_{2.5} = -100.4*C-105.6$
	AORB	$N_fR_{2.5} = 66.00*C + 7.851$	$N_fR_{2.5} = 7.200*C + 4.778$	$N_fR_{2.5} = -10.98*C + 7.293$
N_{f5}	BORB	$N_{f5} = 87.0*C + 167.9$	$N_{f5} = 88.8*C + 134.3$	$N_{f5} = 69.5*C + 39.1$
	EORB	$N_{f5} = 71.5*C + 159.8$	$N_{f5} = 64.0*C + 158.3$	$N_{f5} = 50.4*C + 61.8$
	NORB	$N_{f5} = 66.4*C + 167.4$	$N_{f5} = 47.2*C + 177.1$	$N_{f5} = 41.9*C + 76.5$
	AORB	$N_{f5} = 14.1*C + 179.9$	$N_{f5} = 13.7*C + 161.2$	$N_{f5} = 9.60*C + 98.9$
N_fR_5	BORB	$N_fR_5 = 36.94*C-12.35$	$N_fR_5 = 35.30*C-23.58$	$N_fR_5 = 23.59*C-40.46$
	EORB	$N_fR_5 = 30.83*C-17.85$	$N_fR_5 = 25.00*C-6.306$	$N_fR_5 = 17.00*C-27.13$
	NORB	$N_fR_5 = 28.38*C-12.68$	$N_fR_5 = 17.90*C + 7.259$	$N_fR_5 = 13.97*C-18.49$
	AORB	$N_fR_5 = 6.108*C-4.150$	$N_fR_5 = 5.480*C-4.196$	$N_fR_5 = 3.252*C-5.346$

from effective evaluation indicators. The rejuvenation efficiency of rejuvenators significantly differs from parameter to parameter. Interestingly, the variation trends of parameters αR, kR, and BR are similar, following the AORB (BORB) > NORB > EORB ranking. To these three parameters, the AORB binder shows a lower rejuvenation percentage at low rejuvenator dosages (<7.5%) but a higher value than the BORB when the rejuvenator content is higher than 7.5%. Based on these three parameters, it is difficult to completely distinguish the rejuvenation efficiency of bio-oil and aromatic-oil rejuvenators on the fatigue performance of aged bitumen.

As expected, the bio-oil exhibits the largest rejuvenation efficiency on the $G^*\sin\delta_{initial}$, followed by engine-oil and naphthenic-oil, while the aromatic-oil shows the lowest effect. However, the $G^*\sin\delta_{initial}$ parameter is the fatigue parameter of bitumen without damage, which has been considered and discussed in the LVE fatigue section. Furthermore, the difference in S_fR values of various rejuvenated binders is detected, showing a BORB > EORB(NORB) > AORB ranking. The finding agrees well with the previous conclusion, but the S_fR sequence of EORB and NORB depends on the rejuvenator dosage. In other words, the S_f parameter can reflect the difference in bio-oil and aromatic-oil rejuvenation efficiency but shows limitations in distinguishing the effect of engine-oil and naphthenic-oil in the entire range of rejuvenator dosage. Interestingly, the conclusion on the parameter S_f is exactly complementary to parameters α, k, and B. To differentiate the rejuvenation effectiveness of different rejuvenators on fatigue performance recovery of aged bitumen with LAS parameters, the parameters S_f and α are recommended as complementary evaluation indicators.

4.3. TS test parameters

4.3.1. Aging influence on TS fatigue parameters

The G*-N curve is the main output from the time sweep test, which of fresh and aged bitumen at two stress of 2.5% and 5% are shown in Fig. 21(a). Different important evaluation parameters can be derived from the G*-N curves, such as the fatigue life with 50% residue G* ($N_{50\%}$) and phase angle at the peak point (δ_{peak}). Meanwhile, the dissipated energy ratio (DER) variation versus load cycles (illustrated in Fig. 21(b)) can be used to determine two parameters (fatigue life N_{p20} and initial dissipated energy W_0). The aging effects on these TS fatigue parameters are also plotted in Fig. 21. As the load cycle prolongs, the G* value of bitumen decreases gradually, which is more significant at high strain. Moreover, the descent rate of the G* value becomes faster after long-term aging. High strain level results in a large δ_{peak} value of bitumen, decreasing significantly due to aging.

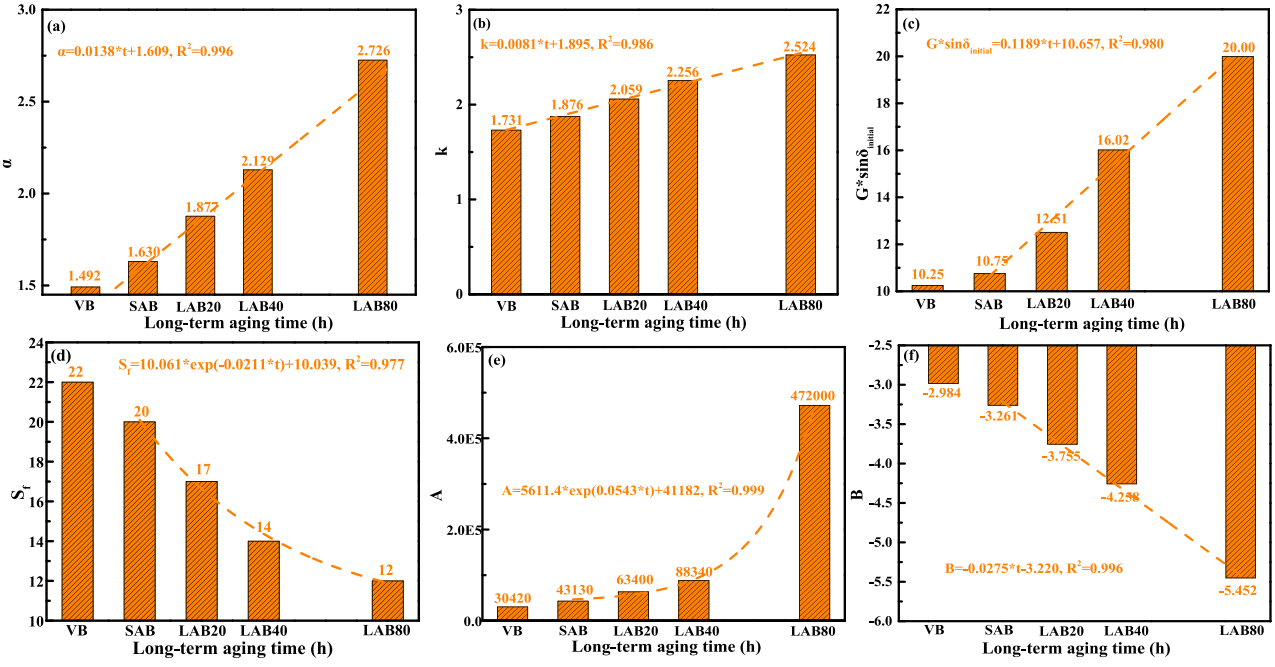

Fig. 19. Aging influence on LAS parameters of bitumen.

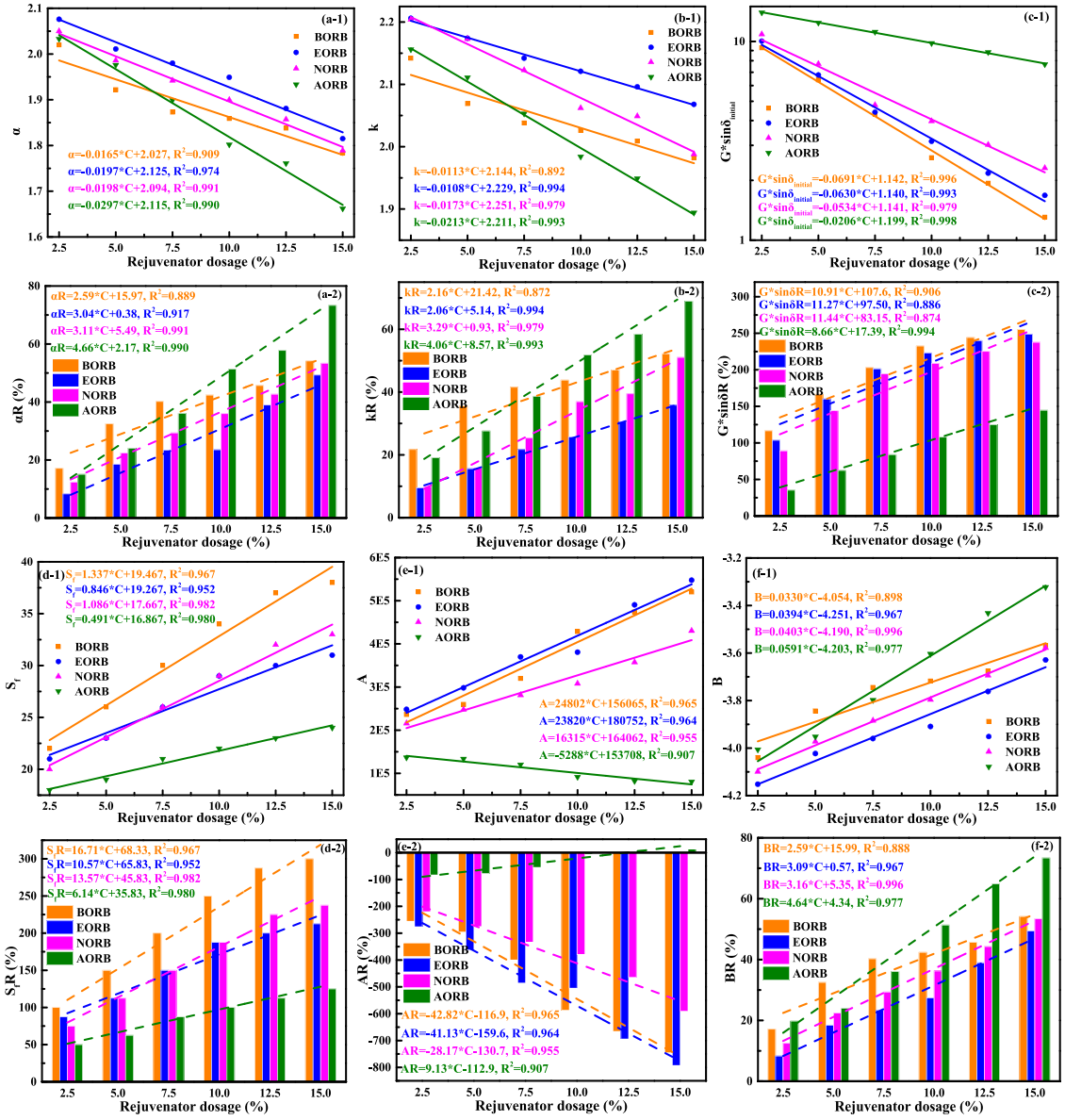

Fig. 20. Rejuvenation influence on LAS parameters of bitumen.

Regarding the DER-N curves, the high strain and aging intensify the increasing rate of DER curves dramatically, reducing the derived N_{p20} value of bitumen. Regardless of the strain levels, the linear relationships between the aging time with parameters $N_{50\%}$, δ_{peak}, N_{p20}, and W_0. Long-term aging reduces the $N_{50\%}$, δ_{peak}, and N_{p20} values but increases the W_0 parameter of bitumen. It suggests that a high aging level significantly shortens the fatigue life, enlarges the elastic ratio, and increases the energy dissipation of bitumen. Further, the high strain decreases the $N_{50\%}$ and N_{p20} and expands the δ_{peak} and W_0 values of bitumen, which weakens the sensitivities of $N_{50\%}$, N_{p20}, and W_0 parameters to the aging time.

4.3.2. TS fatigue parameters of rejuvenated bitumen

Fig. 22 shows the $N_{50\%}$, δ_{peak}, and their rejuvenation percentage ($N_{50\%}R$ and $\delta_{peak}R$) of rejuvenated bitumen. As the rejuvenator dosage increases, the $N_{50\%}$ and δ_{peak} values of rejuvenated bitumen enlarge, showing the opposite trend to the aging effect. It means that the inclusion of rejuvenators improves fatigue life and restores the viscoelastic property of aged bitumen. Like the LAS results, the strain level strongly affects the N50% and N50%R values of rejuvenated bitumen. When the strain level is 2.5%, the $N_{50\%}$-C (and $N_{50\%}R$-C) curves of EORB and NORB binders almost overlap, resulting in huge difficulty in differentiating the rejuvenation efficiency of engine-oil and naphthenic-oil rejuvenators on fatigue life. At 5% strain, the magnitude of $N_{50\%}R$ for rejuvenated binders is EORB > NORB > BORB > AORB. Additionally, the δ_{peak} and $\delta_{peak}R$ values of AORB are the highest, while the NORB shows the lowest values. Nevertheless, the sequence in δ_{peak} and $\delta_{peak}R$ of BORB and EORB inverts as the strain level changes from 2.5% to 5%.

In addition, the results of N_{p20} and W_0 parameters of rejuvenated binders are displayed in Fig. 23. Similar to $N_{50\%}$, several intersections in N_{p20}-C and $N_{p20}R$-C curves of BORB with EORB and NOBR binders at low strain of 2.5%. The variation law of N_{p20} and $N_{p20}R$ versus rejuvenator dosage and type at 5% strain is similar to the $N_{50\%}$ and $N_{50\%}R$ results. However, the ranking of $N_{50\%}R$ and $N_{p20}R$ of rejuvenated binders (EORB > NORB > BORB > AORB) from the TS test differs from N_f from the LAS test (BORB > EORB > NORB > AORB). The reason may be that the $N_{50\%}$ and N_{p20} parameters are determined from G*-N curves without considering the phase angle variation during the TS fatigue test. With the W_0 parameter, the rejuvenation efficiency of rejuvenators can be evaluated and distinguished, which completely agrees with the LVE

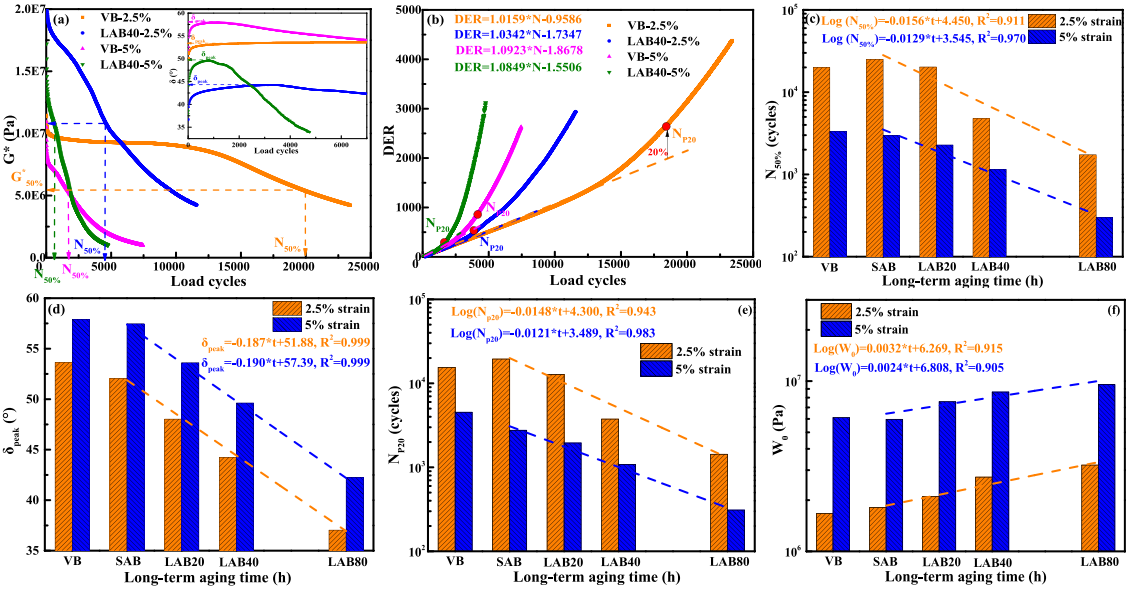

Fig. 21. The TS fatigue parameters of fresh and aged bitumen.

and LAS fatigue results. However, it should be mentioned that the Wo represents the initial dissipated energy without considering the entire fatigue cracking process. These four parameters fail to assess the rejuvenation efficiency of various rejuvenator-aged bitumen blends. The crack-based parameters derived from the TS test will be discussed further in the following subsection.

4.3.3. *Influence of aging on fatigue crack characteristics of bitumen*

The dissipated strain energy (DSE) density is popular to quantify the fatigue potential of bituminous materials, which is defined as the loop area of a stress–strain curve [35]. The DSE density at a given radial position r of undamaged bitumen follows:

$$DSE_0(r) = \int_{t_0}^{t_0+\frac{2\pi}{\omega}} \tau(t)d\gamma(t) = \pi\tau_0(r)\gamma_0(r)\sin\delta_0 = \pi\tau_0(r)^2\frac{\sin\delta_0}{G_0^*} \tag{17}$$

where τ and γ refer to the shear stress and strain; τ_0 and γ_0 are the strain amplitude and stress amplitude; t is the loading time; G^*_0 and δ_0 represent the complex shear modulus and phase angle of undamaged bitumen.

Similarly, the DSE density at the Nth load cycle (DSE_N) of a damaged bitumen can be calculated using Eq.18.

$$DSE_N(r) = \int_{(N-1)\frac{2\pi}{\omega}}^{N\frac{2\pi}{\omega}} \tau_N(t)d\gamma_d(t) = \pi\tau_N(r)\gamma_d(r)\sin\delta_N = \pi\tau_N(r)^2\frac{\sin\delta_N}{G_N^*} \tag{18}$$

where G^*_N and δ_N are the complex shear modulus and phase angle of damaged bitumen at the Nth load cycle.

At the same time, the torque amplitude (T_0 and T_N) on undamaged and damaged bitumen specimens are defined as follows:

$$T_0 = \int_0^{r_0} (\tau_0 \bullet 2\pi r \bullet r)dr = \int_0^{r_0} (\frac{r}{r_0} \bullet \tau_{0max} \bullet 2\pi r \bullet r)dr = \frac{\pi r_0^3}{2}\tau_{0max} \tag{19}$$

$$T_N = \int_0^{r_0} (\tau_N \bullet 2\pi r \bullet r)dr = \int_0^{r_0} \left(\frac{r}{r_0} \bullet \tau_{Nmax} \bullet 2\pi r \bullet r\right)dr = \frac{\pi r_0^3}{2}\tau_{Nmax} \tag{20}$$

where r and r_0 are the radius position and the whole bitumen radius; τ_{0max} and τ_{Nmax} represent the maximum shear amplitude of undamaged and damaged samples at the Nth load cycle, respectively.

Based on the torque amplitude equilibrium principle, the T_N value of damaged bitumen at the Nth load cycle is equivalent to the T_o of undamaged bitumen with an effective radius r_E ($T_N = T_E$), which is displayed as:

$$\frac{\pi r_0^3}{2}\tau_{Nmax} = \frac{\pi r_E^3}{2}\tau_{Emax} \tag{21}$$

where r_E and τ_{Emax} are the effective radius and effective maximum stress amplitude for the undamaged configuration.

The dissipated strain energy (DSE_N) is equivalent to the effective dissipated strain energy (DSE_E), shown in Eqs. (21) and (22).

$$\iiint DSE_N(r)dV_0 = \iiint DSE_E(r)dV_E \tag{22}$$

$$\int_0^{r_0} (\pi\tau_N(r)^2\frac{\sin\delta_N}{G_N^*} \bullet 2\pi r \bullet h)dr = \int_0^{r_E} (\pi\tau_E(r)^2\frac{\sin\delta_0}{G_0^*} \bullet 2\pi r \bullet h)dr \tag{23}$$

where V_0 and V_E are the whole volume of undamaged bitumen and the effective volume of damaged bitumen; h shows the height of the bitumen specimen. Solving Eqs.21 and 23, the crack length c at the Nth load cycle can be calculated as follows:

$$c = r_0 - r_E = \left[1 - \left(\frac{\frac{G_N^*}{\sin(\delta_N)}}{\frac{G_0^*}{\sin(\delta_0)}}\right)^{\frac{1}{4}}\right] r_0 \tag{24}$$

Fig. 24(a) and (b) display the crack morphology and width variation versus load cycles. After fatigue tests, three regions are detected for damaged bitumen: edge flow, factory-roof, and uncracked zones [36], also reflected by the C-N curve. This study compares the C-N curves of fresh/aged and rejuvenated binders with variable rejuvenator conditions. The crack width-based rejuvenation percentage CR is adopted to quantitatively reflect the impacts of rejuvenator type/dosage and aging level on the fatigue cracking of rejuvenated bitumen.

Fig. 24(c) and (d) depict the C-N curves of fresh and aged bitumen at 2.5% and 5% strain levels, respectively. As the load cycle increases, the crack width of bitumen prolongs. The crack growth rate of bitumen increases significantly as the aging degree deepens. In other words, the higher the aging degree of bitumen, the earlier its fatigue failure occurs, especially when the aging level changes to LAB40 and LAB80. Meanwhile, the crack width and growth rate of bitumen both enlarge as the fatigue strain level increases from 2.5% to 5%. At the 5% strain, the crack width of the LAB80 binder increases to 2 mm when the load cycle is 1500, which reaches the half point of the specimen radius (4 mm). In

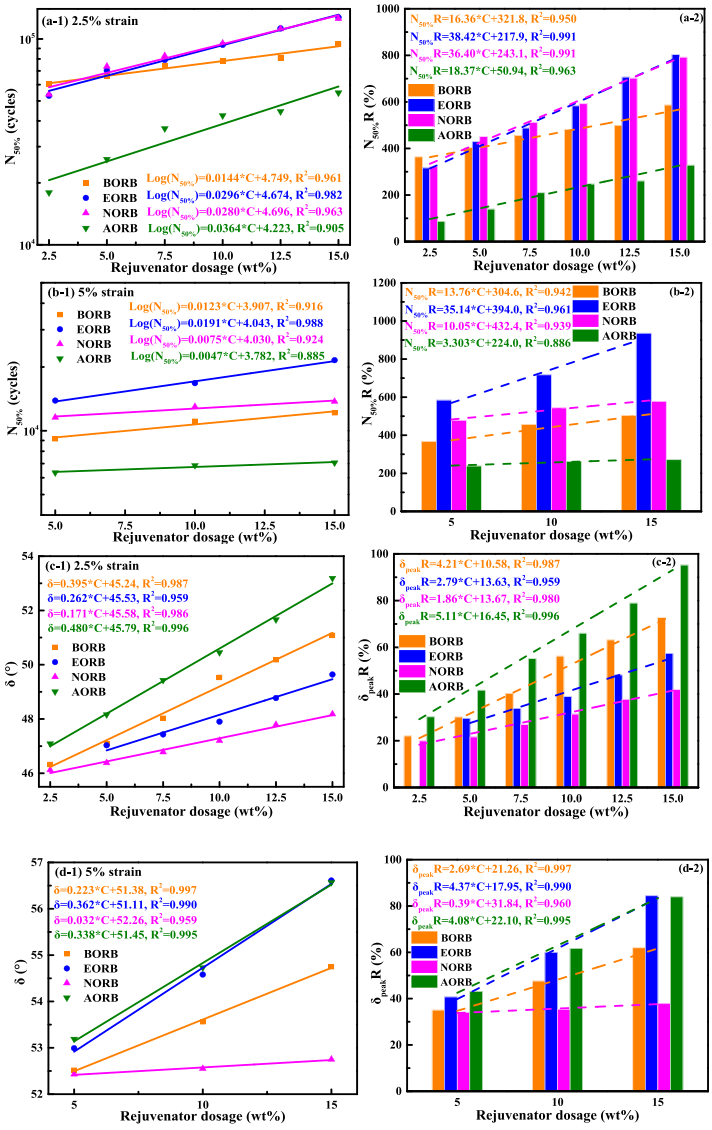

Fig. 22. $N_{p50\%}$, $N_{p50\%}R$, δ_{peak}, and $\delta_{peak}R$ values of rejuvenated bitumen.

this study, the crack width values of fresh/aged and rejuvenated binders at the load cycles of 500, 1500, and 3000 are measured to estimate the aging and rejuvenation effects on the cracking potential of bitumen.

4.3.4. *Fatigue crack characteristics of rejuvenated bitumen*

The C-N curves of rejuvenated binders with different rejuvenator types and dosages at 2.5% and 5% strain levels are displayed in Fig. 25. The fatigue crack initiation and propagation stages are observed. The variation trends of C-N curves of rejuvenated bitumen are slightly influenced by rejuvenator type/dosage. As the rejuvenator dosage increases, the crack width reduces distinctly in the whole region of load cycles. It indicates that the addition of rejuvenators reduces the cracking potential of bitumen. Moreover, the crack width of rejuvenated binders with different rejuvenator types differs significantly. When the rejuvenator dosage and load cycle are fixed, the crack width values of bio-oil rejuvenated bitumen are the smallest, but the aromatic-oil rejuvenated bitumen shows the largest crack degree. The cracking potentials of engine-oil and naphthenic-oil rejuvenated binders are in the middle, and the former is slightly lower than the latter. The increased strain level signally enlarges the crack width of rejuvenated bitumen. The crack growth law of rejuvenated binders is affected by many factors, such as the aging degree of bitumen, rejuvenator type/dosage, strain level, etc. Thus, this study only focuses on the C-N curves within the load cycles of 0–3000.

Table 7 lists the crack width values of fresh/aged and rejuvenated bitumen at the load cycles of 500, 1500, and 3000 to explore the rejuvenation efficiency of various rejuvenators on the potential cracking reduction of aged bitumen with changeable aging degrees. The increased strain level, aging degree, and load cycle all enlarge the crack width of bitumen. Nevertheless, the inclusion of rejuvenators significantly reduces the crack width of aged bitumen regardless of the strain level and load cycle.

The crack width-based rejuvenation percentages of different rejuvenated binders are calculated and illustrated in Fig. 26. All CR values of rejuvenated bitumen show linearly increasing correlations with the rejuvenator dosage. The variation trends of CR-C curves at different load cycles are similar, and thus one crack width parameter is enough to evaluate the rejuvenation efficiency of rejuvenators on cracking potential. Moreover, it is difficult to differentiate the CR values of EORB and NORB at a strain of 2.5%, and the intersections in their C_{1500}-C and C_{3000}-C curves at a 5% strain level are detected. On the contrary, the $C_{500}R$ values can reflect the difference in the rejuvenation effectiveness of these four rejuvenators on the crack width of aged bitumen in the entire dosage range. Therefore, the C_{500} parameter is recommended as

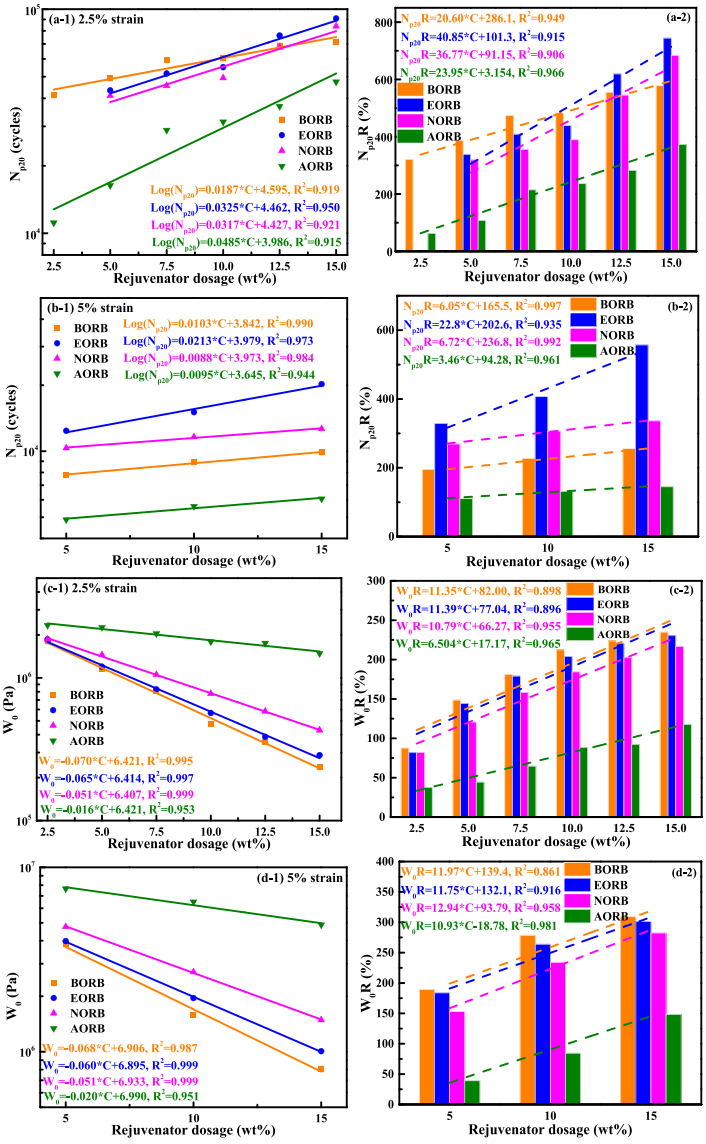

Fig. 23. N_{p20}, $N_{p20}R$, W_0, and W_0R values of rejuvenated bitumen.

an effective indicator for crack width-based fatigue performance evaluation of different rejuvenator-aged bitumen systems. Based on the $C_{500}R$ values, the ranking of crack width reduction efficiency of four rejuvenators is bio-oil > engine-oil > naphthenic-oil > aromatic-oil, which completely agrees with the conclusions from LVE and LAS tests.

As shown in Fig. 27, the CR values of rejuvenated binders strongly depend on the aging degree of bitumen. All CR parameters tend to decrease exponentially as the aging level of bitumen increases. It means that the rejuvenation efficiency of all rejuvenators on preventing the fatigue crack of aged bitumen weakens becomes smaller to an aged bitumen after severe aging. However, the aging degree does not influence the rejuvenation efficiency ranking on crack width reduction of these four rejuvenators. The correlations between the CR values and aging time are beneficial to predict the crack width of rejuvenated bitumen with other aging degrees. According to the results, the C_{500} parameter is preferred to assess the rejuvenation efficiency on crack width restoration of different rejuvenator-aged bitumen blends.

4.4. Critical fatigue evaluation indicators and correlations

Based on the database in this study, several critical fatigue indicators from the linear viscoelastic (LVE) test, linear amplitude sweep (LAS) test, and time sweep (TS) test. From the LVE test, the fatigue failure temperature (FFT) parameter is proposed as an effective LVE fatigue indicator. In the LAS test, the effective indicators are N_{f5}, ε_{sr}, and E parameters. It should be mentioned that the parameters α and S_f derived from the VECD model exhibit a complementary effect on evaluating and differentiating the fatigue life of different rejuvenator-aged bitumen blends. In the TS test, the crack width (C) findings are consistent with conclusions from LVE and LAS tests, which have no significant dependence on the load cycle. Overall, the proposed indicators for effectively evaluating and discriminating the rejuvenation efficiency of rejuvenators on fatigue performance are FFT from LVE, N_{f5}, ε_{sr}, E from LAS, and C_{500} from the TS test.

Exploring the potential connections between these critical evaluation indicators from different fatigue tests is interesting. Fig. 28 depicts the correlation curves between the C_{500} with FFT, N_{f5}, ε_{sr}, and E parameters. The crack width connects well with these parameters, and thus the crack width can be predicted with these correlation equations without conducting the time-consuming time sweep test. As the crack width increases, the FFT values of fresh/aged and rejuvenated binders enlarge while the N_{f5} and ε_{sr} decrease exponentially. Additionally, the elastic modulus E derived from the LAS stress–strain curve behaves in a linearly positive relationship with the C_{500} parameter.

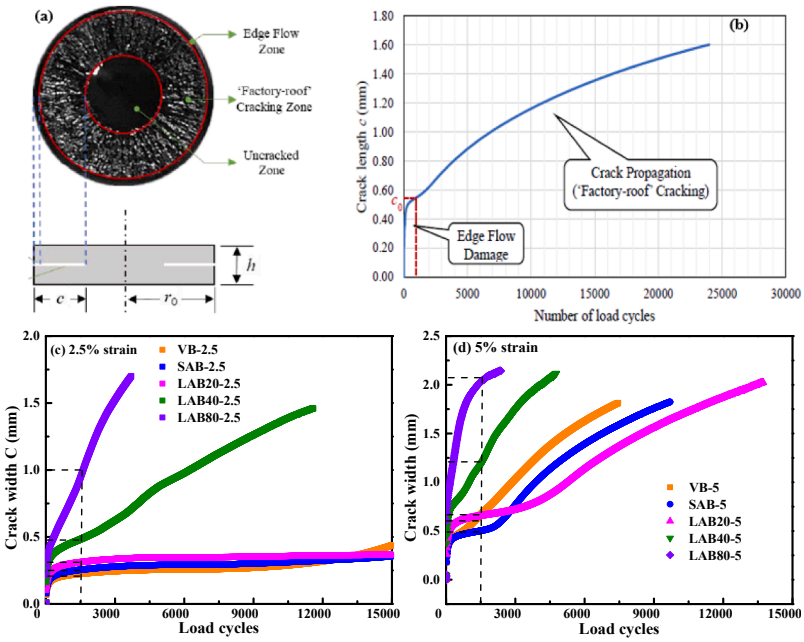

Fig. 24. Fatigue crack characteristics of fresh and aged bitumen.

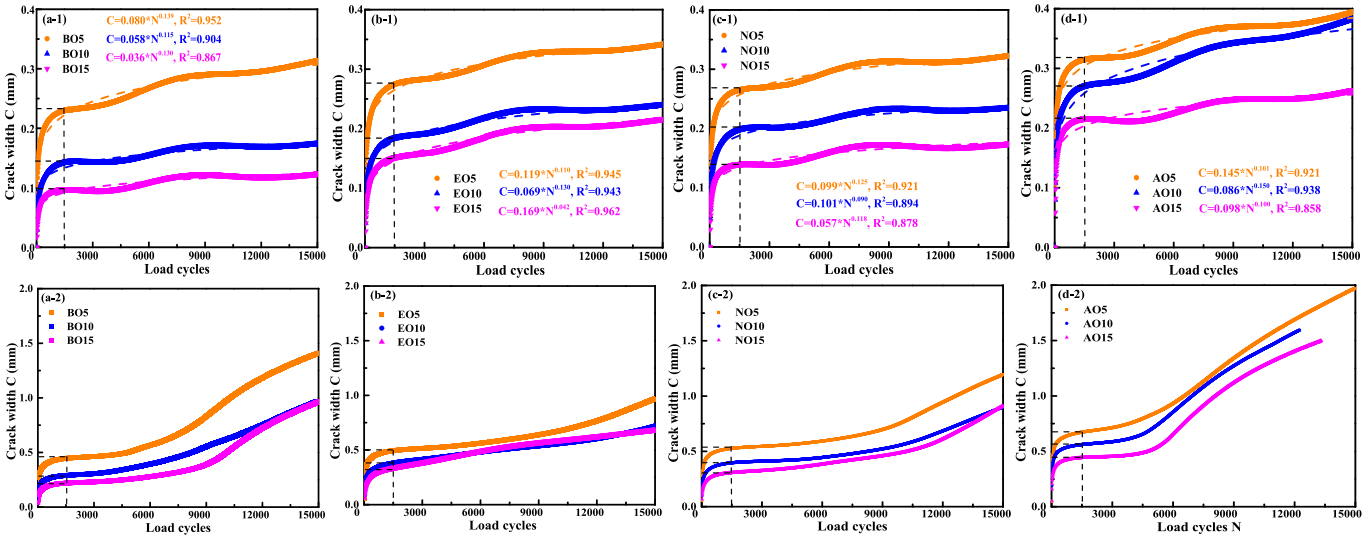

Fig. 25. The crack width curves of rejuvenated bitumen, 2.5% strain: (a-1), (b-1), (c-1), (d-1); 5% strain: (a-2), (b-2), (c-2), (d-2).

5. Conclusions and recommendations

This study proposes critical indicators for effectively evaluating and differentiating the rejuvenation efficiency of various rejuvenators on the fatigue behavior of aged bitumen. Moreover, the potential connections between these proposed fatigue indicators from different fatigue measurements are explored. The main conclusions and some recommendations are as follows:

5.1. Conclusions

(1) The bio-oil exhibits the greatest rejuvenation efficiency in improving the fatigue life of aged bitumen, followed by the engine-oil, naphthenic-oil, and aromatic-oil rejuvenators. Meanwhile, the rejuvenation percentages on fatigue parameters enhance significantly with increased rejuvenator dosage but weaken as the aging level deepens.

(2) From the LVE test, the fatigue parameter (G*sinδ) can better reflect and distinguish the rejuvenation efficiency of various rejuvenators on the LVE fatigue performance of aged bitumen than the G-R parameter, but it shows a limitation of high temperature dependence. The fatigue failure temperature (FFT) parameter is proposed as an effective LVE fatigue indicator.

(3) In the LAS test, the effective indicators are fatigue life (N_{f5}), peak strain (ε_{sr}), and elastic modulus (E) parameters. Moreover, the parameters α and S_f derived from the VECD model exhibit a complementary effect on evaluating and differentiating the fatigue life of rejuvenator-aged bitumen blends.

(4) In the TS test, the parameters $N_{50\%}$ and N_{p20} derived from G*-N and DER-N curves fail to completely distinguish the rejuvenation effects of all rejuvenator-aged bitumen systems due to the negligence of variation in viscoelastic proportion. However, the crack width (C) findings are consistent with conclusions from LVE and LAS tests.

Table 7
The crack width values of fresh, aged, and rejuvenated bitumen.

Bitumen samples		C(N = 500), mm		C(N = 1500), mm		C(N = 3000), mm	
		2.5%	5.0%	2.5%	5.0%	2.5%	5.0%
VB		0.1973	0.4621	0.2244	0.6686	0.2439	1.0337
LAB20		0.2745	0.5943	0.3122	0.6526	0.3355	0.7178
LAB40		0.3998	0.8186	0.4827	1.1761	0.6230	1.7446
LAB80		0.5594	1.4822	0.9432	2.0307	1.5243	2.2124
	BO10	0.0853	0.2016	0.0945	0.2472	0.0891	0.2848
	EO10	0.1272	0.2398	0.1452	0.2791	0.1441	0.3225
LAB20	NO10	0.1428	0.2673	0.1616	0.2976	0.1609	0.3093
	AO10	0.1779	0.2604	0.1876	0.3009	0.1812	0.3193
	BO5	0.2062	0.4030	0.2299	0.4456	0.2359	0.4624
	BO10	0.1228	0.2568	0.1419	0.2893	0.1421	0.3055
	BO15	0.0861	0.1909	0.0977	0.2192	0.0956	0.2305
	EO5	0.2390	0.4431	0.2921	0.4933	0.4225	0.5146
	EO10	0.1604	0.3263	0.1837	0.3798	0.1904	0.4134
	EO15	0.1280	0.2737	0.1518	0.3289	0.1596	0.3759
LAB40	NO5	0.2402	0.4797	0.2650	0.5270	0.2699	0.5452
	NO10	0.1721	0.3523	0.1976	0.3965	0.2009	0.4106
	NO15	0.1244	0.2697	0.1401	0.3056	0.1394	0.3238
	AO5	0.2898	0.6154	0.3146	0.6725	0.3186	0.7134
	AO10	0.2420	0.5174	0.2696	0.5607	0.2761	0.5868
	AO15	0.1962	0.4077	0.2161	0.4415	0.2134	0.4514
	BO10	0.2009	0.3896	0.2330	0.4448	0.2445	0.4700
LAB80	EO10	0.2566	0.4796	0.3043	0.5643	0.3319	0.6395
	NO10	0.2551	0.5120	0.2919	0.5826	0.3074	0.6272
	AO10	0.3215	0.6797	0.3522	0.7397	0.3618	0.7705

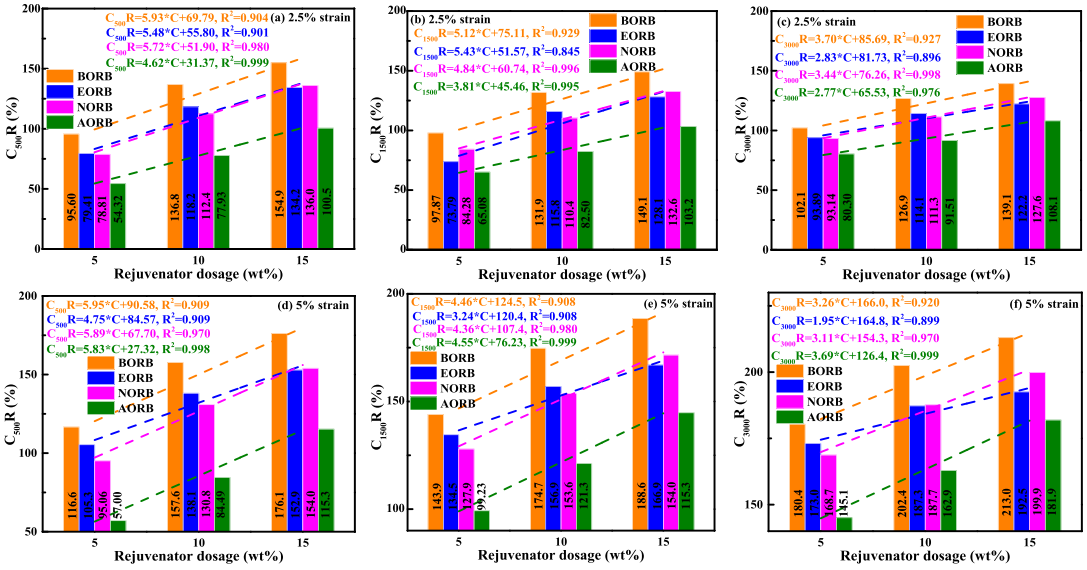

Fig. 26. Crack width and its rejuvenation percentage of rejuvenated bitumen.

(5) The crack width C_{500} parameter shows great correlations with other critical indicators and can be predicted with these correlation equations without conducting the time-consuming time sweep test.

5.2. Recommendations for future work

(1) The critical fatigue parameters evaluating the rejuvenation efficiency of rejuvenated bitumen must be further validated and optimized with more rejuvenation cases.
(2) Implementing the multi-scale exploration of underlying mechanisms on the difference in rejuvenation percentages based on the critical fatigue indicators is important.
(3) The crack initiation and propagation models of fresh/aged/rejuvenated bitumen will be established to fully understand the influence of rejuvenator type/dosage and aging degree.
(4) The potential connections between these fatigue parameters and physicochemical properties (e.g., surface energy and work of cohesion) of rejuvenated binders will be examined.

CRediT authorship contribution statement

Shisong Ren: Methodology, Investigation, Formal analysis, Writing – original draft, Writing – review & editing. **Xueyan Liu:** Supervision, Writing – review & editing. **Sandra Erkens:** Methodology, Supervision.

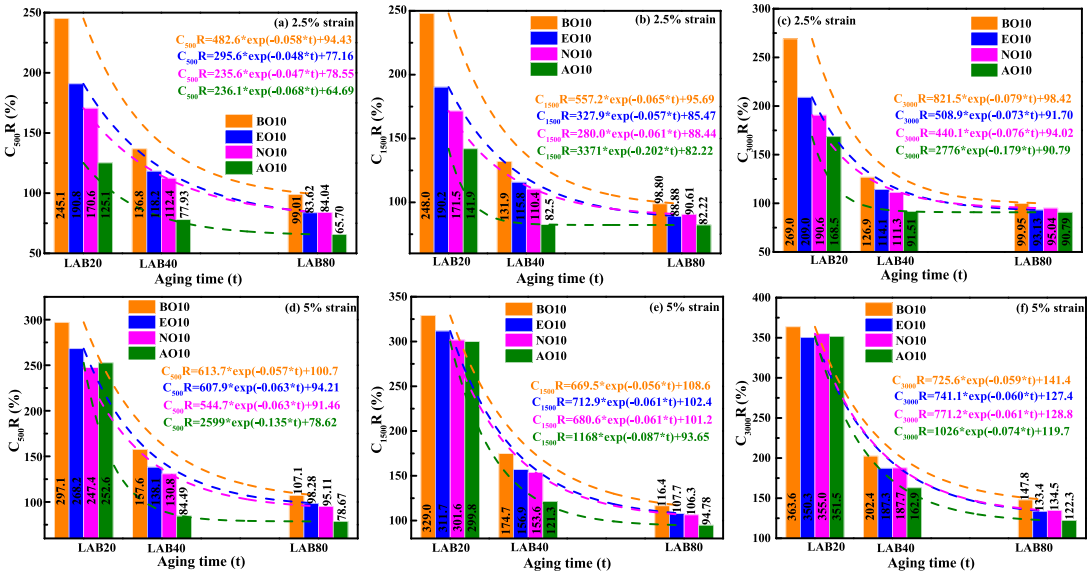

Fig. 27. Influence of aging level on C and CR values of rejuvenated bitumen.

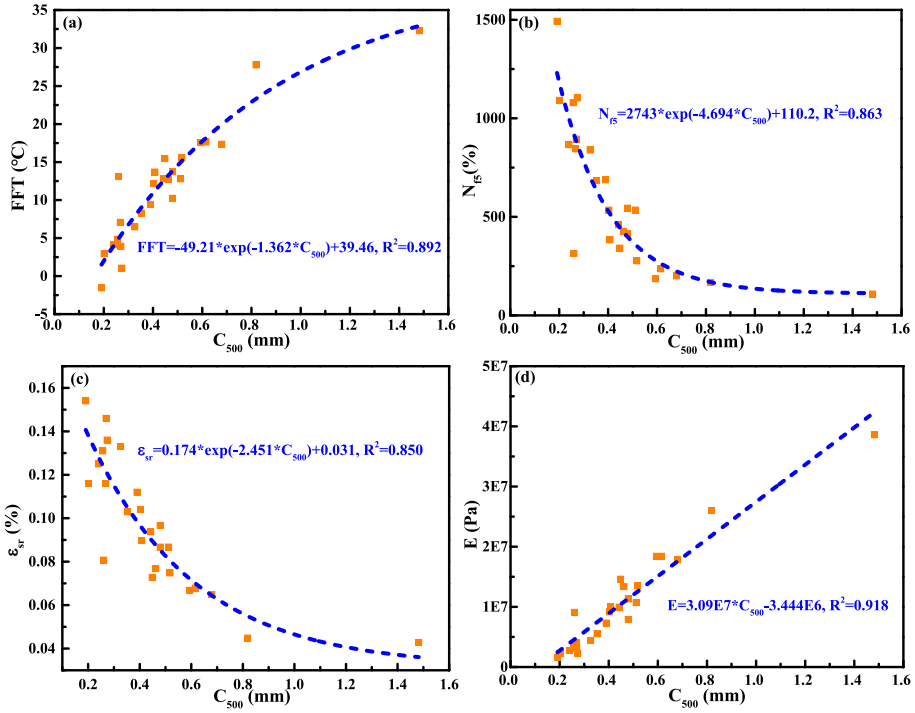

Fig. 28. Correlations between the critical fatigue evaluation indicators.

Declaration of Competing Interest

The authors declare that they have no known competing financial interests or personal relationships that could have appeared to influence the work reported in this paper.

Data availability

Data will be made available on request.

Acknowledgement

The first author would thank the China Scholarship Council for the funding support (CSC, No.201906450025).

Appendix A. Supplementary data

Supplementary data to this article can be found online at https://doi.org/10.1016/j.ijfatigue.2023.107753.

References

[1] Moghaddam T, Baaj H. The use of rejuvenating agents in production of recycled hot mix asphalt: a systematic review. Constr Build Mater 2016;114:805–16.
[2] Zahoor M, Nizamuddin S, Madapusi S, Giustozzi F. Sustainable asphalt rejuvenation using waste cooking oil: a comprehensive review. J Clean Prod 2021; 278:123304.

[3] Ying P, Pan B. Effect of RAP content on fatigue performance of hot-mixed recycled asphalt mixture. Constr Build Mater 2022;328:127077.
[4] Yang K, Li R, Underwood B, Castorena C. Effect of laboratory oxidative aging on dynamic shear rheometer measures of asphalt binder fatigue cracking resistance. Constr Build Mater 2022;337:127566.
[5] Jiao L, Elkashef M, Jones D, Harvey J. Evaluating fatigue performance of fine aggregate matrix mixes with reclaimed asphalt pavement and rejuvenating agents. Road Mater Pavement Des 2020;1826352.
[6] Zhang Z, Han S, Guo H, Han X, Wu C. Fatigue performance evaluation of recycled asphalt fine aggregate matrix based on dynamic shear rheometer test. Constr Build Mater 2021;300:124025.
[7] Zhang Z, Oeser M. Fatigue response and damage accumulation law of asphalt binder after nonlinear viscoelastic cyclic shear loads. Int J Fatigue 2021;146:106156.
[8] Mainieri J, Singhvi P, Ozer H, Sharma B, Al-Qadi I. Fatigue tolerance of aged asphalt binders modified with softeners. Transp Res Rec 2021;2675(11):1229–44.
[9] Mannan U, Islam M, Tarefder R. Effects of recycled asphalt pavements on the fatigue life of asphalt under different strain levels and loading frequencies. Int J Fatigue 2015;78:72–80.
[10] Lopez-Montero T, Miro R, Botella R, Perez-Jimenez F. Obtaining the fatigue laws of bituminous mixtures from a strain sweep test: effect of temperature and aging. Int J Fatigue 2017;100:195–205.
[11] Mangiafico S, Sauzeat C, Benedetto H, Pouget S, Olard F, Planque L. Complex modulus and fatigue performance of bituminous mixtures with reclaimed asphalt pavement and a recycling agent of vegetable origin. Road Mater Pavement Des 2017;18(2):315–30.
[12] Cao X, Wang H, Cao X, Sun W, Zhu H, Tang B. Investigation of rheological and chemical properties asphalt binder rejuvenated with waste vegetable oil. Constr Build Mater 2018;180:455–63.
[13] Elkashef M, Williams R. Improving fatigue and low temperature performance of 100% RAP mixtures using a soybean-derived rejuvenator. Constr Build Mater 2017;151:345–52.
[14] Ali A, Mehta Y, Nolan A, Purdy C, Bennert T. Investigation of the impacts of aging and RAP percentages on effectiveness of asphalt binder rejuvenators. Constr Build Mater 2016;110:211–7.
[15] Zaumanis M, Mallick R, Poulikakos L, Frank R. Influence of six rejuvenators on the performance properties of reclaimed asphalt pavement (RAP) binder and 100% recycled asphalt mixtures. Constr Build Mater 2014;71:538–50.
[16] Santos F, Faxina A, Soares S. Soy-based rejuvenated asphalt binders: impact on rheological properties and chemical aging indices. Constr Build Mater 2021;300:124220.
[17] Alae M, Xu L, Cao Z, Xu X, Xiao F. Fatigue and intermediate-temperature cracking performance of rejuvenated recycled asphalt binders and mixtures: a review. J Clean Prod 2023;384:135587.
[18] Chen H, Bahia H. Modelling effects of aging on asphalt binder fatigue using complex modulus and the LAS test. Int J Fatigue 2021;146:106150.
[19] Hajj R, Bhasin A. The search for a measure of fatigue cracking in asphalt binders - a review of different approaches. Int J Pavement Eng 2018;19(3):205–19.
[20] Elkashef M, Williams R, Cochran E. Investigation of fatigue and thermal cracking behavior of rejuvenated reclaimed asphalt pavement binders and mixtures. Int J Fatigue 2018;108:90–5.
[21] Guduru G, Goli A, Matolia S, Kuna K. Chemical and performance characteristics of rejuvenated bituminous materials with high reclaimed asphalt content. J Mater Civ Eng 2021;33(1):04020434.
[22] Zhou Z, Gu X, Dong Q, Ni F, Jiang Y. Rutting and fatigue cracking performance of SBS-RAP blended binders with a rejuvenator. Constr Build Mater 2019;203:294–303.
[23] Mirhosseini A, Tahami S, Hoff I, Dessouky S, Ho C. Performance evaluation of asphalt mixtures containing high-RAP binder content and bio-oil rejuvenator. Constr Build Mater 2019;227:116465.
[24] Asadi B, Tabatabaee N, Hajj R. Use of linear amplitude sweep test as a damage tolerance or facture test to determine the optimum content of asphalt rejuvenator. Constr Build Mater 2021;300:123983.
[25] Luo Y, Guo P, Gao J, Meng J, Dai Y. Application of design-expert response surface methodology for the prediction of rejuvenated asphalt fatigue life. J Clean Prod 2022;379:134427.
[26] Yang K, Li R, Castorena C, Underwood B. Correlation of asphalt binder linear viscoelasticity (LVE) parameters and the ranking consistency related to fatigue cracking resistance. Constr Build Mater 2022;322:126450.
[27] Cao W, Wang Y, Wang C. Fatigue characterization of bio-modified asphalt binders under various laboratory aging conditions. Constr Build Mater 2019;208:686–96.
[28] Zhao K, Wang W, Wang L. Fatigue damage evolution and self-healing performance of asphalt materials under different influence factors and damage degrees. Int J Fatigue 2023;171:107577.
[29] Yan C, Yuan L, Yu X, Ji S, Zhou Z. Characterizing the fatigue resistance of multiple modified asphalts using time sweep test, LAS test and elastic recovery test. Constr Build Mater 2022;322:125806.
[30] Ncat. NCAT researchers explore multiple user of rejuvenators asphalt technology news 26(1) (2014) 1–16.
[31] Wang H, Liu X, van de Ven M, Lu G, Erkens S, Skarpas A. Fatigue performance of long-term aged crumb rubber modified bitumen containing warm-mix additives. Constr Build Mater 2020;239:117824.
[32] Ren S, Liu X, Lin P, Erkens S, Gao Y. Chemical characterizations and molecular dynamics simulations on different rejuvenators for aged bitumen recycling. Fuel 2022;324:124550.
[33] Shi Z, Su Q, Kavoura F, Veljkovic M. Uniaxial tensile response and tensile constitutive model of ultra-high performance concrete containing coarse aggregate (CA-UHPC). Cem Concr Compos 2023;136:104878.
[34] Ren S, Liu X, Erkens S, Lin P, Gao Y. Multi-component analysis, molecular model construction, and thermodynamics performance prediction on various rejuvenators of aged bitumen. J Mol Liq 2022;360:119463.
[35] Gao Y, Li L, Zhang Y. Modelling crack initiation in bituminous binders under a rotational shear fatigue load. Int J Fatigue 2020;139:105738.
[36] Gao Y. Multiscale Modelling of Bonding Performance of Bituminous Materials. Aston University; 2019. PhD Thesis.